공학박사학위논문

Modeling and Optimal Design of Natural Gas Liquefaction and Regasification Processes

천연가스 액화 및 재기화 공정의 모형 및 최적 설계

2014년 8월

서울대학교 대학원

화학생물공학부

송 기 욱

Abstract

Modeling and Optimal Design of Natural Gas Liquefaction and Regasification Processes

Kiwook Song

School of Chemical & Biological Engineering

The Graduate School

Seoul National University

Natural gas is the world's fastest-growing fossil fuel, favored for electric power and industrial sectors because of its low carbon intensity and reduced emissions. International natural gas trade is expected to double from 1 trillion cubic meter (tcm) in 2010 to 2 tcm in 2030. Liquefied natural gas (LNG) accounts for a growing share of world natural gas. The core of LNG value chain is the phase change of natural gas that makes it feasible for ship transportation to remote regions.

This thesis addresses modeling and optimal design for LNG value chain and it contains two main processes: one is the liquefaction process in the production plant and the other is the regasification process in LNG receiving terminal. These two processes occupy the main parts in the whole in LNG value chain and are worth to be studied in depth.

This thesis has five main parts. First, modeling and simulation of a liquefaction plant is conducted. Second part proposes a simulation-based optimization methodology, taking full advantage of commercial simulator in process design step. The methodology is applied to a case study of double-expander process optimization to prove its performance. A novel process design of natural gas liquefaction using nonflammable refrigerants is developed in the third part. Safety issue for floating LNG drives interest in minimization of hydrocarbon refrigerants. A new N2O-N2O-N2 cascade liquefaction process with nitrous oxide for the pre-cooling and condensation section and nitrogen gas for the sub-cooling section is proposed. Lastly, retrofit design scheme is introduced for boil-off gas handling process in LNG receiving terminal.

Keywords: Process design, optimization, natural gas, LNG, liquefaction plant, LNG Terminal,

Student ID: 2008-21083

Contents

List of Figures

List of Tables

CHAPTER 1 : Introduction

1.1. Research motivation

World natural gas consumption in 2010 was 113.0 tcf (trillion cubic feet) or 3.2 tcm (trillion cubic meters) according to U.S. Energy Information Administration.[1] Natural gas is the fastest-growing fossil fuel in the world with consumption expected to be 185.0 tcf in 2040. Natural gas is favored as an environment-friendly fuel with low carbon intensity and reduced emissions of SOx, NOx and particulates.

Liquefied natural gas (LNG) is a form of natural gas trade together with pipeline transportation, especially important for East Asia such as Japan, South Korea and Taiwan. International LNG trade is expected to double from about 10 tcf in 2010 to about 20 tcf in 2040. New liquefaction plants are planned to be added online mainly in Australia for the next few years and North America will take the lead in the long term. Also LNG importing countries are growing very fast, from 15 countries participating in 2006 to 29 countries in 2013. World LNG trade is not only growing in numbers but also geographically expanding. [2, 3]

LNG value chain starts from exploration & production and then liquefaction, transportation, storage, regasification and distribution follows. The underlying principle of the value chain lies in the practical application of natural gas phase change in liquefaction and regasification processes. Liquefaction of natural gas reduces the volume substantially and makes transportation viable through shipping. However cryogenic energy necessary for the liquefaction requires huge amount of compressor power consumption. In LNG receiving terminals, boil-off gas handling is the key issue to minimize the operating cost. Therefore it is the role of academic

approach of process design and simulation derived from process system engineering to design new processes with safety, reliability and efficiency and to develop process optimization methodology for LNG processing.

1.2. Research objectives

The scope of this thesis is to apply process design and simulation technique to LNG value chain. The objectives of the research are to construct steady state models and develop optimal process design applied to natural gas liquefaction cycles and regasification process. To achieve the objectives, a new methodology for process optimal design utilizing the advantages of simulation is proposed. The methodology is applied to case study of natural gas liquefaction process design. Then a new liquefaction process considering safety issues for offshore application is developed. The novel process is intended to use only nonflammable refrigerants but still increase the efficiency by taking advantage vapor compression refrigeration system. For LNG receiving terminal, concept of retrofit design for existing boil-off gas handling process is proposed to utilize the cryogenic energy of LNG and minimize the operating cost.

1.3. Outline of the thesis

First, modeling and simulation of liquefaction cycles are covered in Chapter 2 with some fundamental background explanation. Chapter 3 proposes a simulation-based optimization methodology for natural gas liquefaction process design. Then in Chapter 4, a novel process of turbine-based liquefaction plant using nonflammable refrigerants is developed. Chapter 5 suggests the retrofit design methodology of a boil-off gas handling process in LNG receiving terminals with a case study. Lastly, in Chapter 6, conclusions and an outline of future works are presented.

CHAPTER 2 : Modeling and Simulation of Liquefaction Cycles* [4]

2.1. Introduction to LNG processing

2.1.1. LNG value chain

LNG value chain is well described in Figure 2-1. Exploration and production step of natural gas from gas field is followed by natural gas liquefaction plant. Natural gas is liquefied and sub-cooled at the plant. Liquefaction plant consists of gas pretreating section (acid gas removal, dehydration, mercury removal, scrubbing, etc.), liquefaction section and fractionation section of the natural gas liquids (NGLs).[5] LNG is shipped using LNG carriers to be transported to importing countries. In the receiving terminal, LNG is offloaded to storage tanks. Then LNG is vaporized to natural gas to be distributed to end user via pipeline. The core of the LNG value chain is to reduce the volume of the natural gas by 1/600 through liquefaction to enable transportation to remote demand areas by shipping.

* The partial part of this chapter is taken from the author's published paper in the journal. [4]

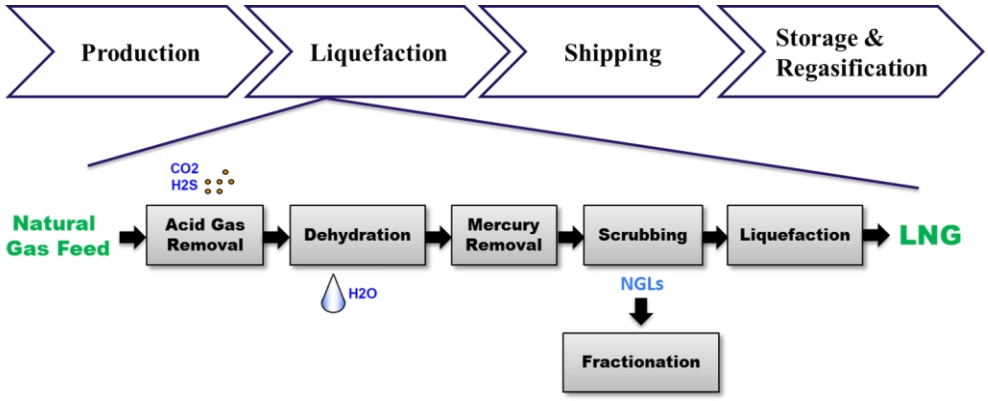

Figure 2- 1. Schematic diagram of LNG value chain.

2.1.2. State of LNG industry

Global LNG trade in 2013 was 236.8 MT (million tons). Qatar was by far the largest LNG exporter while Japan was the main importer. 17 countries participated in LNG supply and export in 2013. Meanwhile, 29 importers received LNG for domestic use which is almost double of 15 in 2006. The number of countries with LNG receiving terminals is increasing quickly and notably geographic spread of international trade is expanding with South American and Middle Eastern non-traditional regions are newly participating. For some countries such as Japan and Korea, LNG is utilized to meet almost the entire gas consumption. It is no surprise that Japan and Korea held 48% of global regasification capacity at the end of 2013.

Average yearly growth rate of LNG demand since 2000 is 7.5%, fairly high compared to 4% of pipeline imports and 1.8% for domestic production. In 1990, LNG made up 4% of global gas demand but now it has grown to 10%. Global nominal liquefaction capacity was 290.7 MTPA (million tons per annum) at the end of 2013. Liquefaction capacity is expected to see rapid growth ahead with 117 MTPA having reached FID (final investment decision) and 626 MTPA of proposed capacity. Short term growth is coming from Australia while long term growth is coming from North America, especially driven by shale gas production. [1]

2.1.3. Floating LNG

Advent of floating LNG (FLNG) can have a potentially transformative impact on LNG industry. LNG-FPSOs (floating production storage and offloading) are suitable for mid-scale or small-scale gas reserves. Unlike conventional large-scale LNG plants, mid-scale and small-scale reserves are more likely to be offshore than onshore. Also, LNG-FPSOs can be repeatedly used for stranded gas resources.[6-13]

The first project to reach FID (final investment decision) was the 3.6 MTPA Prelude LNG project in Australia in 2011. It is expected to be online in 2017. Using Shell DMR process, consortium of Technip and Samsung Heavy Industries is constructing the largest ship ever. [14, 15]

The 1.2 MTPA PETRONAS FLNG project in Malaysia reached FID in 2012. It is expected to be online in 2015, making it the first FPSO producing LNG. Consortium of Technip and Daewoo Shipbuilding & Marine and Engineering (DSME) is building the FPSO with APCI AP-N^{TM} process for liquefaction. AP-N^{TM} process is turbine-based process using nitrogen gas. [16]

The 0.5 MTPA Pacific Rubiales LNG in Colombia reached FID in 2012 also.

In 2014, a fourth FLNG project reached FID: the 1.5 MTPA Rotan FLNG in Malaysia. A consortium of JGC and Samsung Heavy Industries is building the ship also utilizing APCI AP-N^{TM} for topside.

2.2. Liquefaction Cycles

2.2.1. Vapor compression refrigeration

Vapor compression refrigeration is the most common refrigeration system in use for both commercial and industrial application.[17] A simple refrigeration cycle of vapor compression system consists of compressor, evaporator, expansion valve and condenser. Ignoring irreversibility within the evaporator and condenser, the refrigerant flows through the two heat exchangers with no frictional pressure drops. If compression occurs with no heat transfer and irreversibility then the compression process is called to be isentropic. With these considerations, the vapor compression refrigeration system (cycle) is demonstrated on the T-s diagram on Figure 2-2.

Process 1-2: Isentropic compression of the refrigerant

Process 2-3: Heat transfer from the refrigerant in the condenser. State 3 is liquid.

Process 3-4: Throttling process using a Joule-Thompson valve to a two-phase liquid-vapor mixture at state 4.

Process 4-1: Heat transfer to the refrigerant in the evaporator. This is where refrigeration occurs using the latent heat of refrigerant.

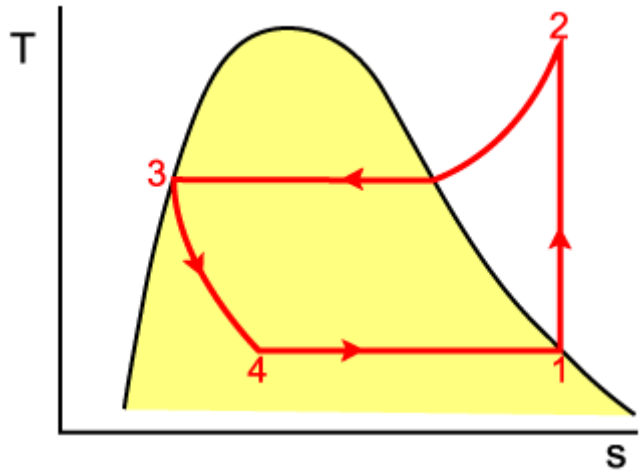

Figure 2- 2. T-s diagram of vapor compression refrigeration cycle.

2.2.2. Gas refrigeration system

Reverse Brayton refrigeration system is an important type of gas refrigeration system. Unlike in vapor compression refrigeration system, the working fluid goes through no phase change and remains a gas throughout the process in gas refrigeration system. These turbine-based processes are well-known for liquefaction of air and other gases used extensively in air separation industry.

The reverse Brayton refrigeration cycle is the reverse of the closed Brayton power cycle. Refrigerant gas enters the compressor and then cooled in the heat exchanger. Then the working fluid is expanded in the expander to achieve very low temperature and refrigeration is achieved through heat transfer from the cold region to the gas in the refrigerator.

For most applications, vapor-compression refrigeration systems are cheaper and operate with higher coefficient of performance than gas refrigeration systems. Compression power requirement for the reverse Brayton cycle is very high even though turbine expansion can provide some auxiliary power.

2.2.3. Natural gas liquefaction processes

Natural gas liquefaction process can be broadly classified into following three groups: [18]

1. Cascade liquefaction processes,
2. Mixed refrigerant processes,
3. Turbine-based processes.

The first two groups are vapor compression refrigeration systems while turbine-based processes are gas refrigeration systems.

Modern base-load plants have a liquefaction capacity of 1 to 8 MTPA (million tons per annum). Among seven major liquefaction technologies employed worldwide, Air Products' propane pre-cooled mixed refrigerant process (C3MR process) [19] remained the most heavily utilized technology in 2013, accounting for 51% of global nameplate capacity. ConocoPhillips' Optimized Cascade® technology [20, 21] is expected to see strong growth from 12% market share in 2013 to 23% by 2018, with main adoption in new plants in US and Australia. Other five major technologies include APC Split MR, APC C3MR/Split MR, APC AP-X, Shell DMR [22] and Linde MFC [23]. Most liquefaction plants utilize mixed refrigerant processes due to relatively high efficiency in terms of compressor power consumption. [24, 25]

Turbine-based liquefaction processes have been preferred for peak shaving plants because of the simplicity and quick startup. [26] Since they have lower efficiency than vapor compression refrigeration systems, they have been rejected to be used in most base-load plants. However they are welcomed for floating LNG (FLNG) due to some advantages such as safety, reliability, easy startup, etc. Both the 1.2 MTPA PETRONAS Kanowit FLNG project and 1.5 MTPA PETRONAS Rotan FLNG

project in Malaysia utilized turbine-based processes using nitrogen as the working fluid (APC AP-N^{TM}). [27]

2.3. Modeling and simulation

Due to computational advances and accumulation of database, accurate modeling of chemical process are achieved using commercial process simulators. Especially Aspen HYSYS® from AspenTech is a comprehensive process modeling tool for oil & gas industry, refineries and engineering companies. Aspen Plus® is also a comprehensive chemical process modeling system for chemical and petrochemical industries. Throughout the thesis, modeling and simulation is conducted using the two commercial simulators. [28]

2.3.4. Mathematical modeling

Mathematical modeling of a simple refrigeration cycle is presented here. It is very important to understand the underlying thermodynamics to design and analyze the liquefaction processes. A basic vapor compression refrigeration cycle is depicted in Figure 2-3. Following assumptions are made for the cycle:

① No pressure drop in the heat exchangers.

② Isentropic compression in compressor.

③ Isenthalpic expansion in expansion valve.

Nomenclature	
h	Specific enthalpy
s	Specific entropy
P	Pressure
v	Molar volume
T	Temperature
q_H	Heat transfer at condenser
q_L	Heat transfer at evaporator
P_{sat}	Saturated pressure
A, B, C	Antoine equation coefficients
v_f	Vapor fraction
Z	Compressibility factor
R	Gas constant
ω	Acentric factor
T_c	Critical temperature
P_c	Critical pressure

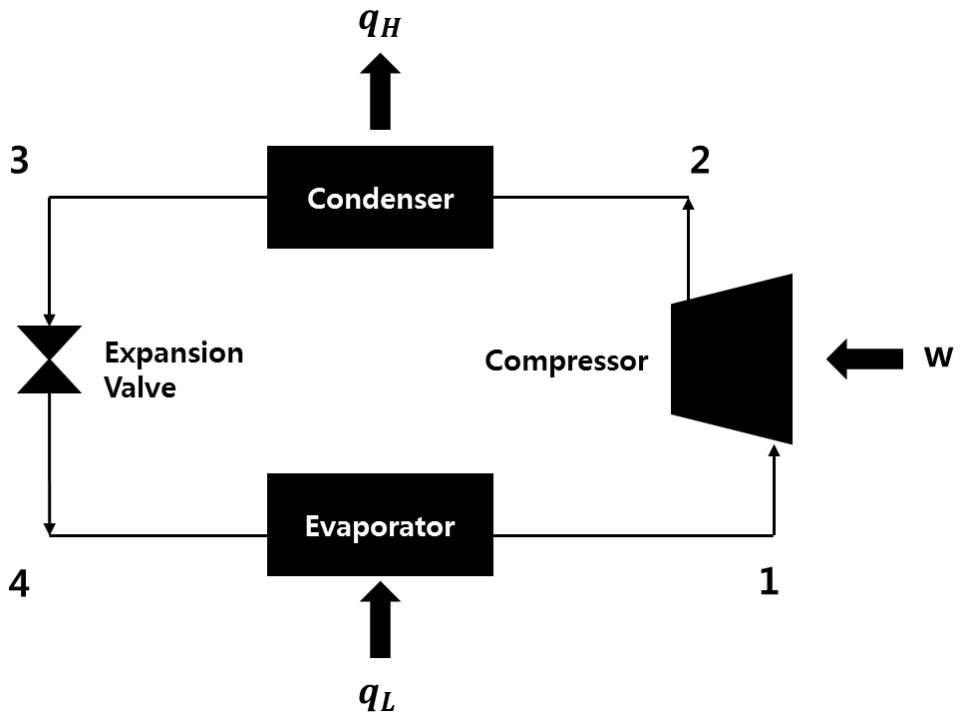

Figure 2- 3. Vapor compression refrigeration cycle.

Compressor:

$$h_1(P_1, v_1, T_1) + w = h_2(P_2, v_2, T_2) \quad (2\text{-}1)$$

$$s_1(P_1, v_1, T_1) = s_2(P_2, v_2, T_2) \quad (2\text{-}2)$$

Condenser:

$$h_2(P_2, v_2, T_2) = q_H + h_3(P_3, v_3, T_3) \quad (2\text{-}3)$$

$$\mathrm{P_2} = \mathrm{P_3} \quad (2\text{-}4)$$

$$\mathrm{P_3} = P_{sat}(T_3) \quad (2\text{-}5)$$

$$\mathrm{P_{sat}} = 10^{A - \frac{B}{T + C - 273.15}} \quad (2\text{-}6)$$

The refrigerant is assumed to be saturated liquid at outlet of condenser. Saturated pressure at the temperature is calculated using the Antoine Equation in Eq. (2-6). [29]

Expansion valve:

$$h_3(P_3, v_3, T_3) = \left(1 - v_f\right) h_{4,l}\left(P_4, v_{4,l}, T_4\right) + v_f h_{4,v}\left(P_4, v_{4,v}, T_4\right) \quad (2\text{-}7)$$

$$\mathrm{P_4} = P_{sat}(T_4) \quad (2\text{-}8)$$

$$v_4 = \left(1 - v_f\right) v_{4,l} + v_f v_{4,v} \quad (2\text{-}9)$$

The refrigerant at the outlet of the expansion valve is liquid-vapor two-phase mixture. The pressure is equal to the saturated pressure at the temperature of the outlet.

Condenser:

$$\left(1 - v_f\right) h_{4,l}\left(P_4, v_{4,l}, T_4\right) + v_f h_{4,v}\left(P_4, v_{4,v}, T_4\right) + q_L = h_1(P_1, v_1, T_1) \quad (2\text{-}10)$$

$$\mathrm{P_4} = \mathrm{P_1} \quad (2\text{-}11)$$

Equation of state (EOS) using cubic equation are generally suitable for modeling hydrocarbon processing. Peng-Robinson (PR) [30] or Soave-Redlich-Kwong (SRK) EOS [31] can be used to correlate densities of gases and liquids to temperature and pressures. A general form of the cubic equation is as follows in Eq. (2-12). Eq. (2-13) and Eq. (2-14) are other forms of Eq. (2-12).

$$\mathrm{P} = \frac{RT}{v-b} - \frac{a(T)}{(v+\varepsilon b)(v+\sigma b)} \tag{2-12}$$

$$\mathrm{Z} = \frac{v}{v-b} - \frac{v}{RT}\frac{a(T)}{(v+\varepsilon b)(v+\sigma b)} \tag{2-13}$$

$$v = \frac{RT}{P} + \mathrm{b} - \frac{v-b}{P}\frac{a(T)}{(v+\varepsilon b)(v+\sigma b)} \tag{2-14}$$

$$\mathrm{a(T)} = \Psi\frac{\alpha(T_r,\omega)R^2T_c^2}{P_c} \tag{2-15}$$

$$\mathrm{b} = \Omega\frac{RT_C}{P_C} \tag{2-16}$$

For PR,

$$\alpha_{PR}(T_r,\omega) = [1 + (0.37464 + 1.54226\omega - 0.26992\omega^2)(1 - T_r^{0.5})]^2 \tag{2-17}$$

For SRK,

$$\alpha_{SRK}(T_r,\omega) = [1 + (0.480 + 1.574\omega - 0.176\omega^2)(1 - T_r^{0.5})]^2 \tag{2-18}$$

Table 2-1 shows the coefficients of general cubic equation for Van der Waals (vdW), Redlich-Kwong (RK), Soave-Redlich-Kwong (SRK) and Peng-Robinson (PR) EOS. [32]

Table 2- 1. Parameters for cubic equation of state.

EOS	$\alpha(T_r)$	σ	ε	Ω	Ψ	Z_C
vdW	1	0	0	1/8	24/64	3/8
RK	$T_r^{-0.5}$	1	0	0.08664	0.42748	1/3
SRK	$\alpha_{SRK}(T_r, \omega)$	1	0	0.08664	0.42748	1/3
PR	$\alpha_{PR}(T_r, \omega)$	$1+\sqrt{2}$	$1-\sqrt{2}$	0.07780	0.45724	0.30740

2.3.5. Modeling and simulation using Aspen HYSYS®

Modeling of the double expander process using nitrogen as the working fluid for natural gas liquefaction is conducted using commercial process simulator, Aspen HYSYS® v7.3. The process is based on US Patent [33] and in-house data for 1 MTPA (million ton per annum) LNG production. The process is modeled using Peng-Robinson property package. Figure 2-4 shows the process flow diagram of the process.

Natural gas feed stream consists of 5.7% of nitrogen, 94.1% of methane and 0.2% of ethane. Streams **1** to **22** are nitrogen streams forming a cycle while **NG1** to **NG7** are natural gas streams. Natural gas and nitrogen inlet temperature values are set to 10℃ using coolers **HX4** and **HX5**, respectively. Double expander process is applied to liquefy the natural gas at 50 bar to -155℃ (Stream **NG6**). Four LNG heat exchanger modules (**LNG-100**, **LNG-101**, **LNG-102**, and **LNG-103**) are used to simulate multi-stream heat exchange.

Natural gas at 50 bar is cooled to -20℃ in **LNG-100** and then liquefied in **LNG-101** with discharge temperature of -90℃. **LNG-101** module is where phase change of natural gas to LNG is occurred. LNG is further cooled to -110℃ and -155℃ at **LNG-102** and **LNG-103**, respectively. LNG is expanded in **JT1** to 1.2 bar resulting in temperature decrease to -165.2℃.

There is no phase change in nitrogen refrigerant and the cycle is operated only in vapor phase. Nitrogen gas is compressed to 55 bar by compressor modules **C1**, **C2**, **C3** and **C4**. Nitrogen after the second stage of compressor (**C2**) is split in **TEE-100** to stream **6** and **8** to be compressed further in **C3** and **C4**, respectively. **HX1**, **HX2**, **HX3** are air coolers to cool down the compressor discharge streams to 30℃. Refrigerant at 10℃ (stream **12**) is precooled with the natural gas feed stream (**NG2**)

to -20℃ in **LNG-100**. Then, the refrigerant is split in **TEE-101** module to stream **14** and stream **16**. Stream **14** is expanded to 9 bar at expander **X1** and is mixed with stream **19** to form stream **20**, a cold stream that liquefies the natural gas in **LNG-102**. Nitrogen in stream **16** is further cooled at **LNG-101** to -90℃ and later expanded to 9 bar at expander **X2**. This cold stream at -159.8℃ is used as the coldest stream to assure the temperature of LNG fall down to -155℃. Turbo expander **X1** is arranged to drive the compressor **C3** and turbo expander **X2** is arranged to drive compressor **C4**. So, power produced from the expanders is recovered in compressors. The compressors need not to be separate units and can be connected to a common shaft.

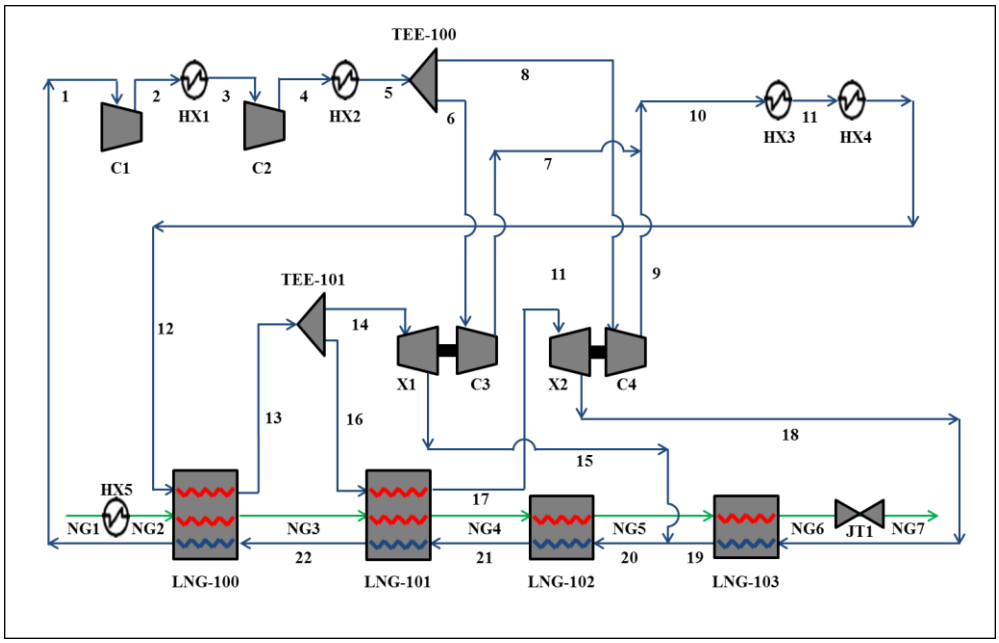

Figure 2- 4. Process flow diagram of natural gas liquefaction plant.

2.3.6. Degree of freedom analysis

Here we calculate potential steady-state operational degree of freedom (DOF) suggested by Jensen and Skogestad. [34] The process shown in Figure 2-4 consists of 2 mixers, 2 splitters, 5 heat exchangers, 4 LNG-exchanger modules, 4 compressor modules, 2 expander modules and one expansion valve. The mixers have no potential DOF. For splitters, the potential DOF is one less than the number of exit streams. In the given process, there are two exit streams for each splitter. So the potential DOF is 2 for the two splitters. For heat exchangers, the potential DOF is 1. When the temperature of all hot exit streams in LNG-exchanger is assumed to be same, the potential DOF for LNG-exchanger module is also 1. The compressor and expander modules have potential DOF of 1. Expansion valve also has a potential DOF of 1. Feed rate of natural gas stream and nitrogen stream adds 2 potential DOF. So the potential DOF of the liquefaction process is 20 in total. The results are summarized in Table 2-2.

Table 2- 2. Potential steady-state operational degree of freedom of the natural gas liquefaction process.

Process Unit	Potential DOF	Total Units	Total Potential DOF
Feed	1	2	2
Mixer	0	2	0
Splitter	1	2	2
Heat Exchanger	1	5	5
LNG-exchanger	1	4	4
Compressor Module	1	4	4
Expander Module	1	2	2
Expansion Valve	1	1	1
Total			20

The following specifications are given to the process:

(1) Feed mass flow rate of natural gas is given.

(2) The outlet temperature of **HX1** is 30℃.

(3) The outlet temperature of **HX2** is 30℃.

(4) The outlet temperature of **HX3** is 30℃.

(5) The outlet temperature of **HX4** is 10℃.

(6) The outlet temperature of **HX5** is 30℃.

(7) The outlet temperature of **LNG-103** is -155℃.

(8) Expander module **X1** and compressor module **C3** is connected to a common shaft.

(9) Expander module **X2** and compressor module **C4** is connected to a common shaft.

(10) Discharge pressure of **C1** is 22 bar.

(11) Discharge pressure of **C3** is 55 bar.

(12) Discharge pressure of **C4** is equal to the discharge pressure of **C3**.

(13) Discharge pressure of **X1** is equal to the discharge pressure of **X2**.

(14) Discharge pressure of **JT1** is 1.2 bar.

The specifications above are equations that reduce the degree of freedom of the process. So the actual DOF is 20 - 14 = 6.

The 6 design variables are the following:

(1) Refrigerant mass flow rate

(2) Split ratio of **TEE-101**

(3) Discharge pressure of the refrigerant at expander

(4) Discharge temperature of natural gas at **LNG-100**

(5) Discharge temperature of natural gas at **LNG-101**

(6) Discharge temperature of natural gas at **LNG-102**

CHAPTER 3 : Simulation-based optimization methodology for process design with case study of turbine-based liquefaction process*

3.4. Introduction

Commercial process simulators are widely used in both industry and academia for LNG plant modeling. [35-37] Significant progress in computer performance and database construction has led to accurate modeling of complex flowsheets. Process simulators are basically based on first-principle models but usually do not provide gradient information needed for deterministic optimization. Conventional optimization technique when using the process simulator is to integrate with external optimizer such as MATLAB® . Optimization algorithm in external optimizer tool runs the simulator to search optimal point but it fails often to converge and is heavily affected by initial point. Also, models with many recycle loops and design specifications require large computational effort and are time-consuming, particularly not appropriate for on-line applications.

Objective of this chapter is to discuss a solution to simulation-based optimization technique. The main concept is to apply process mapping technology to develop an empirical model that predicts the objective function value and constraint function values. Empirical modeling technique has been applied to fitting process models to industrial data [38-40], development of soft sensors (Kadlec et al. provided a

* The partial part of this chapter is taken from the author's published paper in the journal. [4]

comprehensive review on data-driven soft sensors) [41] and model reduction for real time optimization [42, 43] and monitoring [44, 45]. Previous studies proved that empirical modeling of chemical processes show high prediction performance and can be used as alternative to first-principle models.

A simulation-based optimal design framework applied for natural gas liquefaction plant using double-expander process is proposed in this chapter. Detailed steps of simulation-based optimization framework is introduced in 3.2. Then, base case design of the turbo-expander process is described in 3.3. After determining the design space, an empirical model that predicts the objective function value and constraint function values is developed in 3.4. Finally, results are shown with discussion in 3.5.

3.5. Simulation-based optimization framework

The simulation-based optimization framework to be introduced here is an optimal design technique using commercial process simulators as basic process modeling. Figure 3-1 shows the steps of the proposed technique. The methodology includes process mapping of the design space with empirical modeling. This is to develop a short-cut data-driven model of the target process for the required operation window.

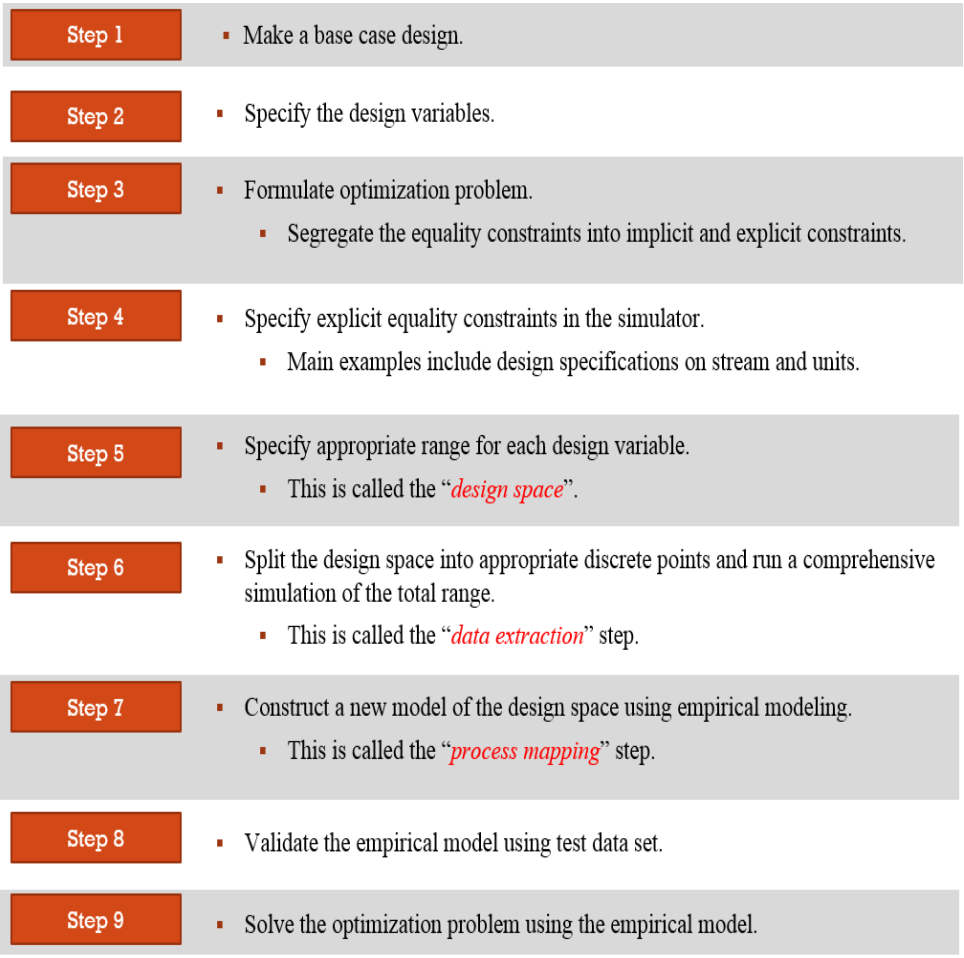

Figure 3- 1. Steps of the simulation-based optimization framework.

Steps in detail are as follows.

Step 1. Make a base case design of the target process with initial design points using the commercial simulator. The base structure of the process will remain fixed throughout the optimization procedure. The process simulator calculates all the mass and energy balance of the flowsheet.

Step 2. Specify the design variables. Design variables are manipulated process variables that are to be optimized. Parameters, dependent variables and independent variables should be determined by the user. Parameters are physical quantities that are fixed at a constant value throughout the simulation and optimization. Independent variables are variables that can be varied by the engineer for simulation and optimization while dependent variables are other variables that are affected by the changes of the independent variables.

Step 3. Formulate the optimization problem by specifying the objective function and constraints. Optimization problem can be written as follows.

$$\text{minize or maximize } z = f(\mathrm{X}) \tag{3-1}$$

$$\text{s.t. } \mathrm{h_I}(\mathrm{X}) = 0 \tag{3-2}$$

$$\mathrm{h_E}(\mathrm{X}) = 0 \tag{3-3}$$

$$\mathrm{g}(\mathrm{X}) \leq 0 \tag{3-4}$$

where X is a vector of design variables.

Eq. (3-1) is the objective function to be minimized or maximized. Equality constraints may be segregated to implicit and explicit constraints. Eq. (3-2) represents a set of

implicit constraints that are met by the simulator, such as material and energy balance. The main advantage of using the simulator in optimal process design is that the implicit equations are always satisfied. Eq. (3-3) represents the explicit equality constraints that are additionally specified in Step 4. Eq. (3-4) represents the inequality constraints and main examples of them include bounds on purity, minimum temperature approach, temperature difference, conversion, selectivity, etc.

Step 4. Specify explicit equality constraints in the process simulator. Design specifications on stream variables such as temperature, pressure or flow rate values are main examples. Specifications on units such as pressure drop, heat duty, reflux ratio, conversion, etc. are also useful. This step is incorporating all the equality constraints into the simulator so that we can later map the design space which always meets the equality conditions.

Step 5. Specify appropriate range for each design variable. This is called the 'design space'. In conventional optimization formulation, design variable range is expressed in inequality form. In our framework, the optimization space is confined to the design space.

Step 6. Split the design space into appropriate discrete points and run a comprehensive simulation of the total range. This is the 'data extraction' step.

Step 7. Construct a new model of the design space using empirical modeling. This is called the 'process mapping' step. The developed empirical model is the short-cut data-driven model of the target process for the design space only. It should not be used for extrapolation. The input variables of the model are the design variables. The model is to predict the objective function value f(X) and inequality constraint

function value g(X). Predicting multivariate outputs is an important feature since the values of inequality constraints should be included in addition to the estimation of the objective function value.

Step 8. Validate the empirical model using test data set. If the empirical model shows reasonable prediction performance then it can be used for optimization.

Step 9. Solve the optimization problem of the process using the developed empirical model.

3.6. Case study of natural gas liquefaction process

3.6.7. STEP 1: Base case design

The process modeled in Chapter 2 (Section 2.3.2) is used as the base case design.

3.6.8. STEP 2: Specifying the design variables

Total of 6 design variables are to be manipulated in the target process. The design variables include the refrigerant mass flow rate (or refrigerant to natural gas ratio), split ratio of **TEE-101** (flow ratio of stream **14**), discharge pressure of the refrigerant at expander (stream **15** or **18**), and discharge temperature values of natural gas at LNG exchangers **LNG-100**, **LNG-101 and LNG-102** (streams **NG3**, **NG4** and **NG5**).

3.6.9. STEP 3: Optimization formulation

Optimization formulation is as follows:

$$\min Z\ (Total\ shaft\ work) \tag{3-5}$$

$$\text{s.t. } h_I(X_D) = 0 \tag{3-6}$$

$$h_E(X_D) = 0 \tag{3-7}$$

$$MTA_k \geq 3 \quad \text{(for k = } \textbf{LNG-100}, \textbf{LNG-101}, \textbf{LNG-102} \text{ and } \textbf{LNG-103}\text{)} \tag{3-8}$$

where X_D is a vector of design variables specified in 3.3.2.

The objective function for optimal design of liquefaction process in Eq. (3-5) is to minimize total shaft work, which means compression work of **C1** and **C2**. The equality constraints in Eq. (3-6) include all the thermodynamic equations together with unit operation equations. Additional equality constraints to be expressed explicitly in Eq. (3-7) will be explained in 3.3.4. The inequality constraints in Eq. (3-

8) represent the minimum temperature approach (MTA) of each LNG exchanger. Here, the lower limit is 3K.

Minimum temperature approach for natural gas liquefaction cold box is usually assumed to be 1-3 K. However, for smaller MTA the heat exchange area becomes bigger. So in the thesis MTA limit is assumed to be 3K. Table 3-1 summarizes the MTA values used in the literature. [18, 35, 46-50]

Table 3- 1. Minimum temperature approach values used in literature for natural gas liquefaction cold box.

Reference	MTA value
Venkatarathnam, 2008. Springer. [18]	3K
Wang et. al., 2011. I&ECR. [35]	2K
Chang et. al., 2011. Cryogenics. [46]	3K
Remeljej and Hoadley, 2006. Energy. [47]	2K
Lee et. al., 2012. I&ECR. [48]	3K
Taleshbahrami and Saffari, 2010. Trans. Can. Soc. Mech. Eng. [49]	3K
Alabdulkarem, 2011. Appl. Therm. Eng. [50]	3K

3.6.10. STEP 4: Providing additional constraints in the simulator

The temperature value of stream **13** is set to be equal to the temperature of stream **NG3**. In addition, the temperature values of stream **17** and **NG4** are set to be equal. The pressure values of stream **15** and **18** are also set to be equal. Pressure values of streams **7** and **9** are also set to be equal and are fixed at 55 bar. The split ratio of **TEE-100** is not a design variable and is rather a variable that is adjusted depending on split ratio of **TEE-101** and expander discharge pressure value. Discharge pressure of **C2** (stream **4**) is also a variable that is adjusted depending on the power recovered in **C3** and **C4**. These design specifications are easily modeled in process simulators.

3.6.11. STEP 5: Determining the design space

Table 3-2 shows the design variables, their initial points and variable range. The design space is the operating window that we are interested in. To minimize the shaft work of compressor, nitrogen flowrate (or refrigerant to natural gas ratio) should be decreased from the initial point. Split ratio of **TEE-101** (flow ratio of stream **14** to stream **16**) should be increased from the initial point to minimize the heat duty of **LNG-101**, which makes it possible to further decrease the refrigerant requirement. Expander discharge pressure value should be increased from the initial point since the compressor discharge pressure is fixed in this case and lower expander discharge pressure results in higher compression ratio and higher power consumption. The outlet temperature value of each LNG exchanger has multiple effects on the process and should be determined by optimization.

Table 3- 2. Design variables and design space of the liquefaction process.

No.	Design variable	Initial point	Lower Bound	Upper Bound	Dimension
1	N2 refrigerant flowrate	1300	1000	1300	[ton/h]
2	Split ratio of TEE-101	0.5	0.5	0.7	-
3	Expander discharge pressure	9	9	12	[bar]
4	LNG-100 outlet temperature	-20	-20	-10	[℃]
5	LNG-101 outlet temperature	-90	-90	-80	[℃]
6	LNG-102 outlet temperature	-110	-120	-110	[℃]

3.6.12. STEP 6: Comprehensive simulation of the design space

The six design variables have lower and upper bounds. The range for each variable is divided into 6 intervals. A comprehensive simulation, that is six to the sixth power, is performed for data extraction. An external operator such as MATLAB® is used for easy handling of data input and output. The data collected are the objective function value and minimum temperature approach values for each LNG exchanger. Therefore, data table of six input variables and five output variables is constructed through comprehensive simulation.

3.6.13. STEP 7: Process mapping of the design space using empirical modeling

An empirical modeling is used for process mapping. Examples of empirical modeling include multiple linear regressions, partial least squares regressions[51], and other useful machine learning methods. Artificial neural network is useful when estimating various output variables from various input variables.[52] ANN is a well-known technique to model nonlinear characteristics applied to a variety of chemical engineering field.[53].

In this study, a feed-forward back-propagation network with one input layer – one hidden layer – one output layer configuration is employed. The input layer consists of 6 nodes, each corresponding to the six design variables. The hidden layer has 20 nodes. The output layer has 5 nodes, one for objective function and 4 for minimum temperature approach value for LNG exchangers. All data are scaled before empirical modeling. Tan-sigmoid function in Eq. (3-9) is used for the activation function.

$$y = \frac{\exp(x)-\exp(-x)}{\exp(x)+\exp(-x)} \quad (3\text{-}9)$$

3.6.14. STEP 8: Empirical modeling validation

Test data set of 5000 randomly sampled observations is utilized for empirical model validation. The model predicts 5 output variables, total shaft work and minimum temperature approach values for each LNG exchanger. Validation of the model means comparing the predicted values with original simulator data. The results show excellent agreement between the simulator and data-driven model. Average error percent and root mean squared error (RMSE) of the values are tabulated in Table 3-3. Average error is less than 0.2% and the difference of simulator and neural network model is negligible. Therefore, the developed empirical model can be utilized as a representative model for the target design space instead of the commercial simulator itself.

It has been shown that empirical modeling of the design space shows great performance of process mapping. However, the prediction performance may vary with dimension of design space, broadness of each input variable range, structure of the empirical model, etc. Process engineers should predefine a tolerance for the prediction error and only use the proposed methodology when the performance of the developed data-driven model is acceptable.

Table 3- 3. Prediction performance of the neural network model.

Output Variable	Average Error	RMSE	Dimension of RMSE
Total shaft work	0.029 %	3.611	[kW]
MTA of **LNG-100**	0.017 %	0.006	[K]
MTA of **LNG-101**	0.014 %	0.043	[K]
MTA of **LNG-102**	0.042 %	0.011	[K]
MTA of **LNG-103**	0.127 %	0.049	[K]

3.6.15. STEP 9: Optimization

For the initial design point, optimization using MATLAB® linked with HYSYS® does not converge to a value and fails to solve the problem. Case studies with different initial points were also performed and the results of conventional optimization showed a high dependence on initial value. However, when the process design space is mapped using the suggested technique, the optimization problem is solved regardless of the starting point. The optimization results are tabulated in Table 3-4.

Table 3- 4. Optimization results of the liquefaction process using proposed methodology.

Category	Variable	Before Optimization	After Optimization	Dimension
Design Variable	N2 refrigerant flowrate	1300	1078	[ton/h]
	Split ratio of TEE-101	0.5000	0.5900	-
	Expander discharge pressure	9.0000	9.6483	[bar]
	LNG-100 outlet temperature	-20.00	-20.00	[℃]
	LNG-101 outlet temperature	-90.00	-85.96	[℃]
	LNG-102 outlet temperature	-110.00	-110.00	[℃]
Objective Function	Total shaft work	57954	45938	[kW]
Constraints	LNG-100 MTA	14.17	3.00	[K]
	LNG-101 MTA	15.53	3.00	[K]
	LNG-102 MTA	15.87	4.71	[K]
	LNG-103 MTA	8.06	3.00	[K]

To finally check the reliability of the empirical model, the optimized values need to be compared with the simulator values. Table 3-5 shows the result and the difference between the empirical model and the simulator is in acceptable range.

The advantage of the proposed optimization framework is that process designers can take full advantage of the process simulators. Process simulators are easy to handle and inherently calculates unit operation equations with vast and accurate thermodynamic database. Also process designers can readily apply many design specifications into the simulator that need some iteration steps to solve.

Table 3- 5. Empirical model and simulator values using the optimized design variables.

Category	Variable	Empirical model	Simulator	Dimension
Design Variable	N2 refrigerant flowrate	1078	1078	[ton/h]
	Split ratio of TEE-101	0.5900	0.5900	-
	Expander discharge pressure	9.6483	9.6483	[bar]
	LNG-100 outlet temperature	-20.00	-20.00	[℃]
	LNG-101 outlet temperature	-85.96	-85.96	[℃]
	LNG-102 outlet temperature	-110.00	-110.00	[℃]
Objective Function	Total shaft work	45938	45941	[kW]
Constraints	LNG-100 MTA	3.00	3.01	[K]
	LNG-101 MTA	3.00	2.98	[K]
	LNG-102 MTA	4.71	4.71	[K]
	LNG-103 MTA	3.00	3.00	[K]

3.7. Comparison with response surface methodology

Response surface methodology (RSM) is a multivariate statistical technique to find the relationship between the response and the independent variables. [54-56] For a well-known linear function the approximation is defined as first-order model as equation (3-10).

$$Y = \beta_0 + \sum_{i=1}^{k} \beta_i x_i \quad (3\text{-}10)$$

Y is the response (yield) and β represents the coefficient and x represents independent variables.

For second-order model, equation (3-11) is used.

$$Y = \beta_0 + \sum_{i=1}^{k} \beta_i x_i + \sum_{i=1}^{k} \beta_{ii} x_i^2 + \cdots + \sum_{i<j} \sum \beta_{ij} x_i x_j \quad (3\text{-}11)$$

Y is the response (yield), β_0 is the constant coefficient, β_i represents the linear coefficients, β_{ii} represents quadratic coefficients and β_{ij} represents the interaction coefficients.

Visualization of the model obtained by the response surface method is represented by surface plot and contour plot. The response surface plot is the three-dimensional plot showing the relationship between the predicted value Y and the independent variables. In the contour plot, lines of constant response are shown in two-dimensional space to visualize the shape of a response surface. Figure 3-2 is an illustrative example of response surface methodology.

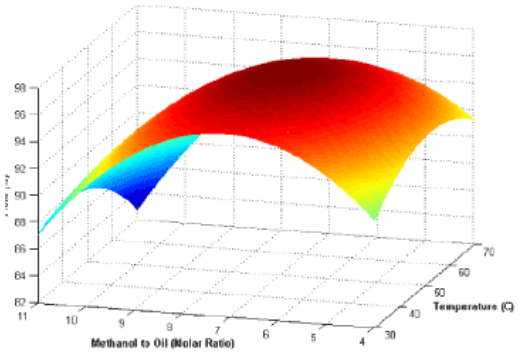

Figure 3- 2. An illustrative example of response surface methodology.

Second-order design methods include the full three-level factorial design, the Box-Behnken design and central composite design (CCD). Full three-level factorial design is a basic experimental matrix calculated by expression $N = 3^k$, where N is the experiment number and k is the number of independent variables. Each variables is equally spaced to three levels so that they correspond to -1, 0, 1. This design consists of all the combinations of the levels of k variables. Because a complete factorial design requires a lot of experimental runs it is not commonly applied in practice. Schematic diagram of full three-level factorial design with three variables is shown in Figure 3-3 (a).

Box and Behnken[57] suggested a more efficient and economical way to select points from the factorial arrangement. It provides three levels for each variable and consists of a subset of factorial combinations. The variables are changed two at a time with all the other variables remaining at their mid levels. The experimental points are located on a hyper sphere equidistant from the central point. For example, Box-Behnken design for three independent variables requires 13 experimental points, while 27 points are needed for full three-level factorial design. Schematic diagram of Box and Behnken design with three variables is shown in Figure 3-3 (b).

The central composite design (CCD) method was suggested by Box and Wilson.[58] This method consists of three parks: (1) a full factorial or fractional factorial design (2) axial points (or α level points) (3) a central point. The axial points are $2k$ points arranged at a distance of α from the design center on the axis of each independent variable. So all factors are studied in five levels $(-\alpha, -1, 0, +1, +\alpha)$. For example, CCD design for three independent variables with two-level factorial and $\alpha = 1.68$ is shown in Figure 3-3 (c).

The optimization framework suggested here has similar concept with the response

surface methodology (RSM). The main difference is the purpose of the technique. RSM is utilized to find an effective experimental design and develop a second-order model to find the optimal point. RSM gives a regression model from a small number of experiments and is useful when the model is unknown. In simulation-based optimization method, the model of the process is already built and the engineer knows all information from the developed model. However, the purpose is to build a short-cut model with the objective function value and the constraint function value as the predicted variables. Also RSM usually uses second-order polynomial to fit the experimental data. But a second-order polynomial is usually not appropriate for process modeling. In the proposed simulation-based optimization model, artificial neural network is used. Lastly, in simulation-based optimization, the simulation is performed in the commercial simulator. Therefore a huge number of the simulation can be performed easily on the computer and a full-factorial design is readily available. When the number of independent variables is large, a more effective way such as Box and Behnken method of central composite design method can be used.

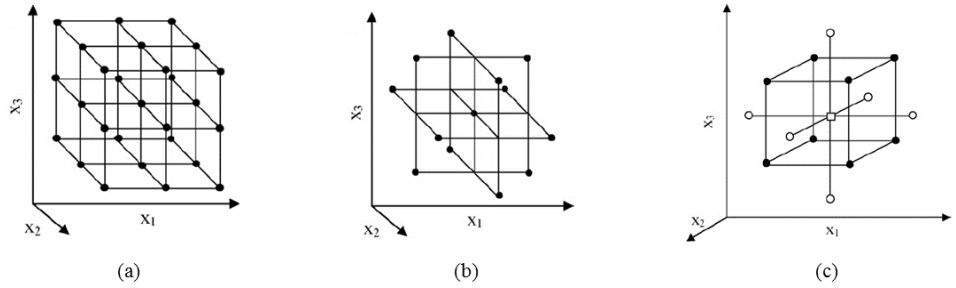

Figure 3- 3. Schematic diagram of second-order design methods: (a) Full factorial design, (b) Box and Behnken design and (c) central composite design.

CHAPTER 4 : Natural gas liquefaction process design with nonflammable refrigerants for offshore application

4.8. Introduction

Global natural gas demand is expected to surge, nurtured by growing preference for low-carbon environment-friendly energies and uncertainty in policies related to nuclear power generation. While conventional scale natural gas plants with reserves of 5 to 100 tcf (trillion cubic feet) are being fully explored and developed, the impetus to monetize mid-scale (0.5 to 5 tcf) and small-scale gas reserves is growing. Especially, offshore floating LNG (FLNG) production is gaining interest since it offers the opportunity to develop smaller or remote fields. LNG-FPSO (Floating production, storage and offloading) employed in offshore natural gas reserves can be repeatedly used for stranded gas resources.

Natural gas liquefaction process for existing base-load plants are mostly based on mixed refrigerant processes or cascade processes, both based on hydrocarbon refrigerants. For FLNG, minimization of flammable inventory is important for safety, driving interest in refrigeration cycles that contain no hydrocarbons. The nitrogen recycle expander plant, well-known and extensively used in air separation industry, is a good alternative for offshore application. Turbine-based processes offer advantages of safety, easy startup and small layout. However, they have been rejected in onshore application due to low efficiency in terms of compression power requirement. [9, 59-61]

To increase the capacity and efficiency of turbine-based processes, modifications of the processes have been proposed. Dubar suggested double and triple expander processes by dividing the refrigerant stream into two or three portions.[62] Dual expander processes proposed by Statoil is a similar concept.[63] Adding a precooling unit is also an option. CO2 precooled dual expander process was suggested by Statoil[64] while Air Product proposed AP-HN processes that use HFC (hydro fluorocarbon) as the precooling refrigerant.

In this chapter, a novel process design of turbine-based natural gas liquefaction plant for offshore application is conducted. To meet the safety criteria for LNG-FPSO, the process utilizes only nonflammable refrigerants, especially nitrous oxide (N2O). First, thermodynamic analysis of carbon dioxide (CO2, R744) and nitrous oxide (N2O, R744a) is performed. Then a cascade process of N2O-N2O-N2 is developed for offshore LNG production application.

4.9. Thermodynamic analysis of carbon dioxide and nitrous oxide

CO2 and N2O are both nonflammable refrigerants that are good candidates for offshore application. Their thermodynamic characteristics are quite similar. Critical point of CO2 is 73.8 bar and 31.3℃ while critical point of N2O is 72.45 bar and 36.37℃. If we neglect supercritical phase and restrict the operating range to sub-critical region, then the critical pressure imposes an upper limit on the compressor discharge pressure in the vapor-compression refrigeration system. Also the critical temperature determines the upper limit of cooling water or air temperature in the condenser. For example, assuming 5K of minimum temperature approach in the condenser, cooling water or ambient air of temperature higher than 26℃ is not appropriate for CO2 condenser. Critical temperature of nitrous oxide is slightly higher than that of carbon dioxide, which makes N2O favorable for flexible selection of condensing working fluid.

Triple point of the refrigerant imposes a lower limit in the operating range of the vapor-compression refrigeration system. Triple point of CO2 is 5.18 bar, -56.56 ℃ and triple point of N2O is 0.8785 bar, -90.82 ℃. Temperature of the triple point of nitrous oxide is much lower than that of CO2, which makes N2O favorable for use in LNG plants.

Typical liquefaction process of natural gas at about 50 bar can be divided into the following three sections:[46]

1. Pre-cooling section in vapor phase (300 – 240 K),
2. Condensation section (240 – 200K),
3. Sub-cooling section in liquid phase (200 – 120K).

Given that the triple point of CO2 is 5.18 bar and -56.56℃, CO2 can only be applied for pre-cooling section. Meanwhile N2O is possible for pre-cooling and condensation section also.

Nitrous oxide (N2O) is a nonflammable and nontoxic gas but needs to be dealt with caution since it is classified as an oxidant.[65] Also careful consideration is needed when selecting the material. Material compatibility from Air Liquide [66] is shown in Table 4-1. The table is recommend to be used to choose possible materials and more extensive investigation and testing must be carried out under the specific conditions of use. Equipment must be thoroughly degreased for nitrous oxide handling and there is risk of violent reaction particularly with the valves.

Table 4- 1. Material compatibility for nitrous oxide.[66]

Material	Compatibility
Aluminum	Satisfactory
Brass	Satisfactory but corrosive in presence of moisture
Copper	Satisfactory but corrosive in presence of moisture
Ferritic Steels (e.g. Carbon Steel)	Satisfactory but corrosive in presence of moisture
Stainless Steel	Satisfactory
Polytetrafluoroethylene (PTFE)	Satisfactory
Polychlorotrifluoroethylene (PCTFE)	Satisfactory

4.10. Design of N2O-N2O-N2 cascade process

For design of natural gas liquefaction cycles, assumptions are given as follows: [47, 48, 59, 67-77]

① Composition of pre-treated clean natural gas feed is as given in Table 4-1.

② Mass flow rate of feed gas is 228 ton/h which corresponds to approximately 2 MTPA (million ton per annum) of LNG production. LNG rundown flowrate is 206.9 ton/h

③ Pressure drop in all heat exchangers (condensers, after-coolers and LNG exchangers) are ignored.

④ Adiabatic efficiency of turbo machinery (compressors and turbines) is 80%.

⑤ Discharge temperature of all condensers and after-coolers is 30℃.

Here we introduce a cascade process of N2O-N2O-N2 refrigerants for natural gas liquefaction. A cycle using N2O is applied for pre-cooling section and a different cycle of using also N2O is applied for condensation section. N2 refrigerant is applied for the sub-cooling section of liquefied natural gas. Cycles with N2O refrigerant is vapor-compression refrigeration system and utilizes the latent heat of the refrigerant. N2 cycle is operated in gaseous phase utilizing sensible heat only. ASPEN HYSYS® v7.3 is used for steady-state simulation using Peng-Robinson property package.

Table 4- 2. Composition of natural gas feed.

Component	Mole Fraction
Nitrogen	0.040
Methane	0.875
Ethane	0.055
Propane	0.021
i-Butane	0.003
n-Butane	0.005
i-Pentane	0.001

4.10.16. Pre-cooling section

N2O refrigerant is utilized in the pre-cooling section to cool down both the refrigerant itself and natural gas to -33℃. The refrigeration cycle is configured as multistage vapor compression refrigeration system with three different expansion stages. Figure 4-1 shows the process flow diagram of the pre-cooling unit. Streams Pre-1 to Pre-21 are N2O refrigerant streams while NG-1 to NG-4 are natural gas streams. The refrigerant is compressed in the compressor modules Pre-C1, Pre-C2 and Pre-C3. Discharge pressure of Pre-C3 is 65 bar and the refrigerant is cooled and condensed in E-101 to ambient temperature 30℃. First expansion pressure at Pre-5 is 35.57 bar, second expansion pressure at Pre-10 is 19.46 bar and third expansion pressure at Pre-14 is 10.65 bar. Pre-5 stream cools NG-1 and Pre-2 streams while evaporation of the refrigerant occurs. Similarly, Pre-10 cools NG-2 and Pre-8. Pre-14 exchanges heat with NG-3, Pre-12 stream and also Con-3 stream of the condensation unit. LNG-109 is a regenerative heat exchanger to cool down Con-2 from 30℃ to -14℃ at Con-3.

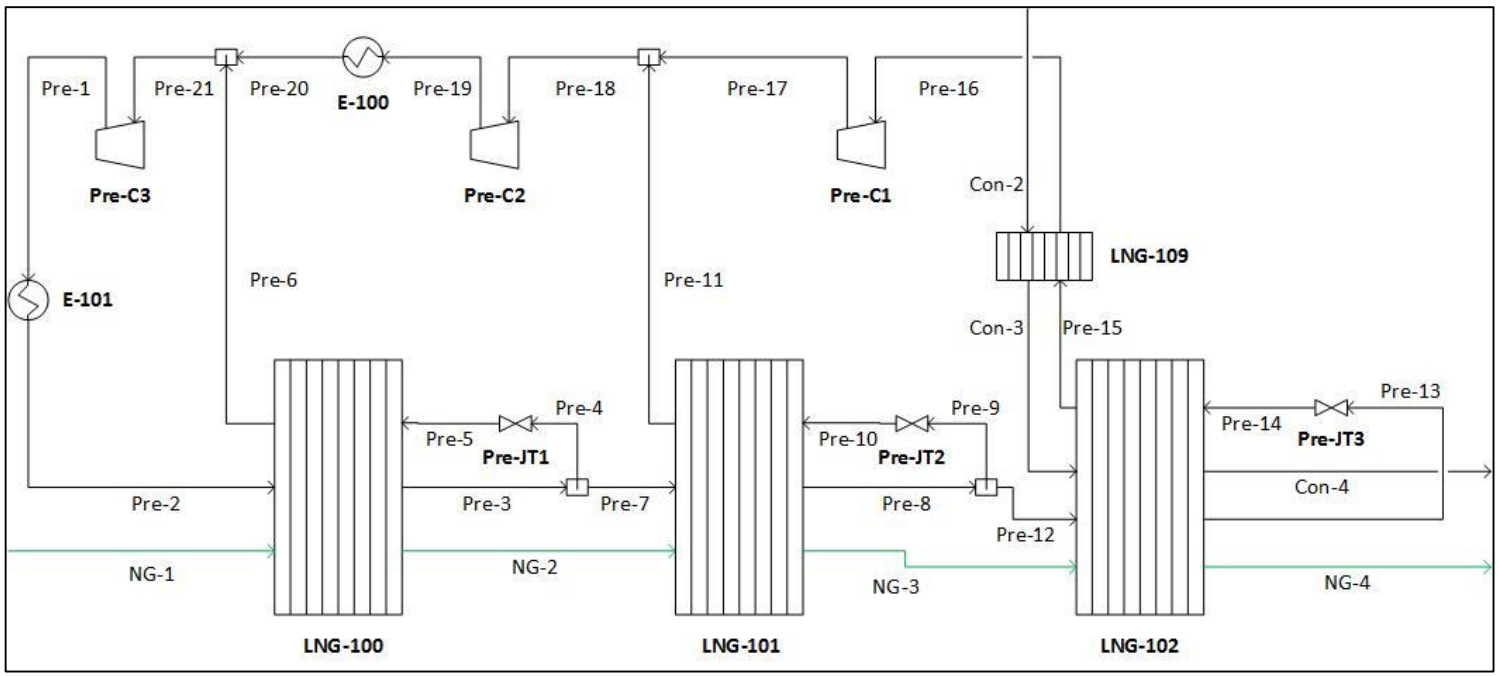

Figure 4- 1. Process flow diagram of the pre-cooling section.

4.10.17. Condensation section

Natural gas is liquefied in the condensation section. The process diagram is depicted in Figure 4-2. The objective of this section is to cool down the natural gas to -78.6℃. The refrigeration cycle with N2O as the working fluid is also configured as multistage vapor compression refrigeration system with three different expansion stages. Streams Con-1 to Con-21 are N2O refrigerant streams while NG-4 to NG-7 are natural gas streams. The refrigerant is compressed in the compressor modules Con-C1, Con-C2 and Con-C3. Discharge pressure of Con-C3 is 12.5 bar and the refrigerant is cooled in E-102, LNG-109 and LNG-102 in series. The boiling temperature of nitrous oxide at 12.5 bar is -31.24℃, Con-4 is liquid phase at -33℃. A portion of the refrigerant is expanded in Con-JT1 to 6.17 bar and cools NG-4 and Con-4 streams using latent heat. Second stage expansion pressure is 3.04 bar while final stage expansion pressure is 1.5 bar in Con-JT3. Con-16 stream at -81.61℃ is used for the liquefaction of natural gas and cooling of Con-14. It also cools down Sub-4 stream of the Sub-cooling unit.

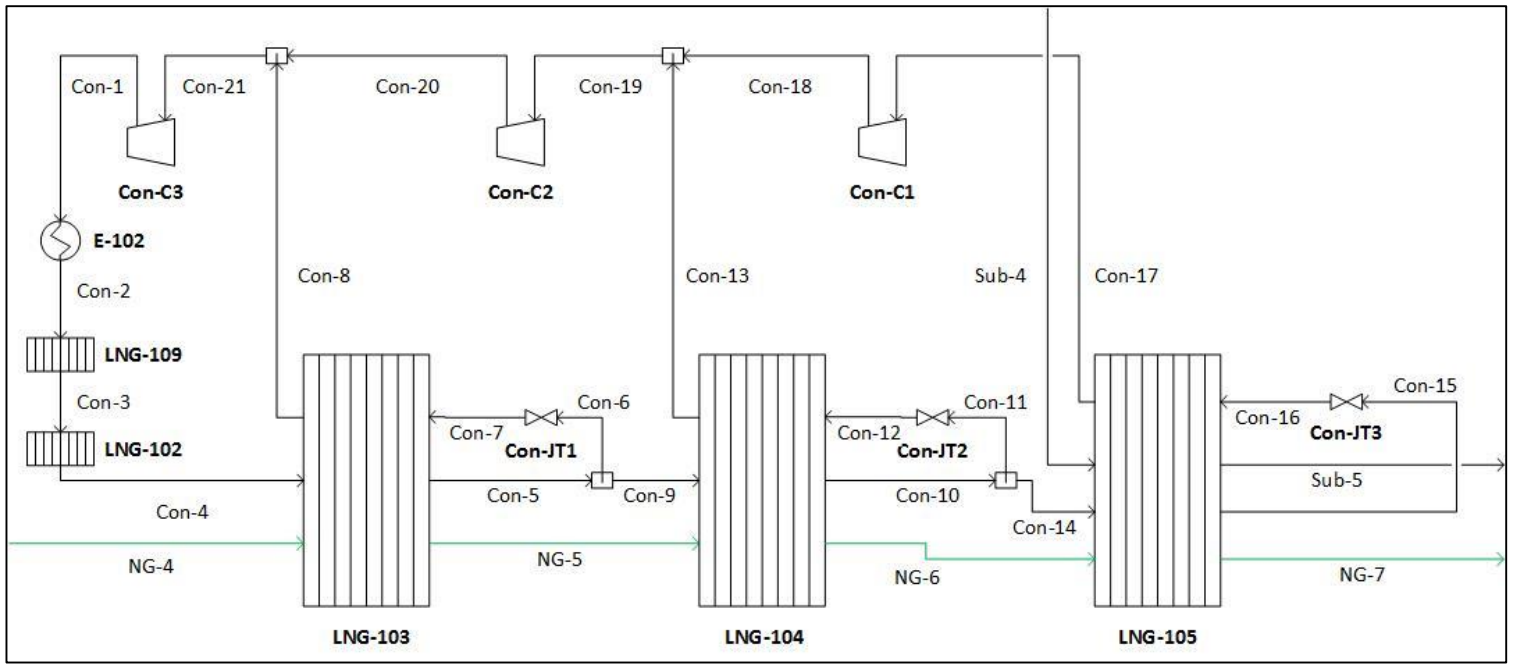

Figure 4- 2. Process flow diagram of the condensation section.

4.10.18. Sub-cooling section

The sub-cooling section in Figure 4-3 is a gas compression refrigeration system where no phase change of the refrigerant occurs. Nitrogen gas is compressed in Sub-C1, Sub-C2 and Sub-C3 to 70 bar and cooled in E-105 to 30℃. E-103 and E-104 are after-coolers with discharge temperature of 30℃. LNG-110 is a regenerative heat exchanger to cool down Sub-2 to -64.51℃ at Sub-3. A portion of Sub-3 goes through expansion in Sub-X2 and utilized as the cold stream in Sub-10. Other portion is cooled in LNG-105 in Condensation unit, further cooled in LNG-106 by nitrogen itself to 124℃ and then expanded in Sub-X1 to 18.1 bar and -158.1℃. This stream is used for sub-cooling LNG to -155℃.

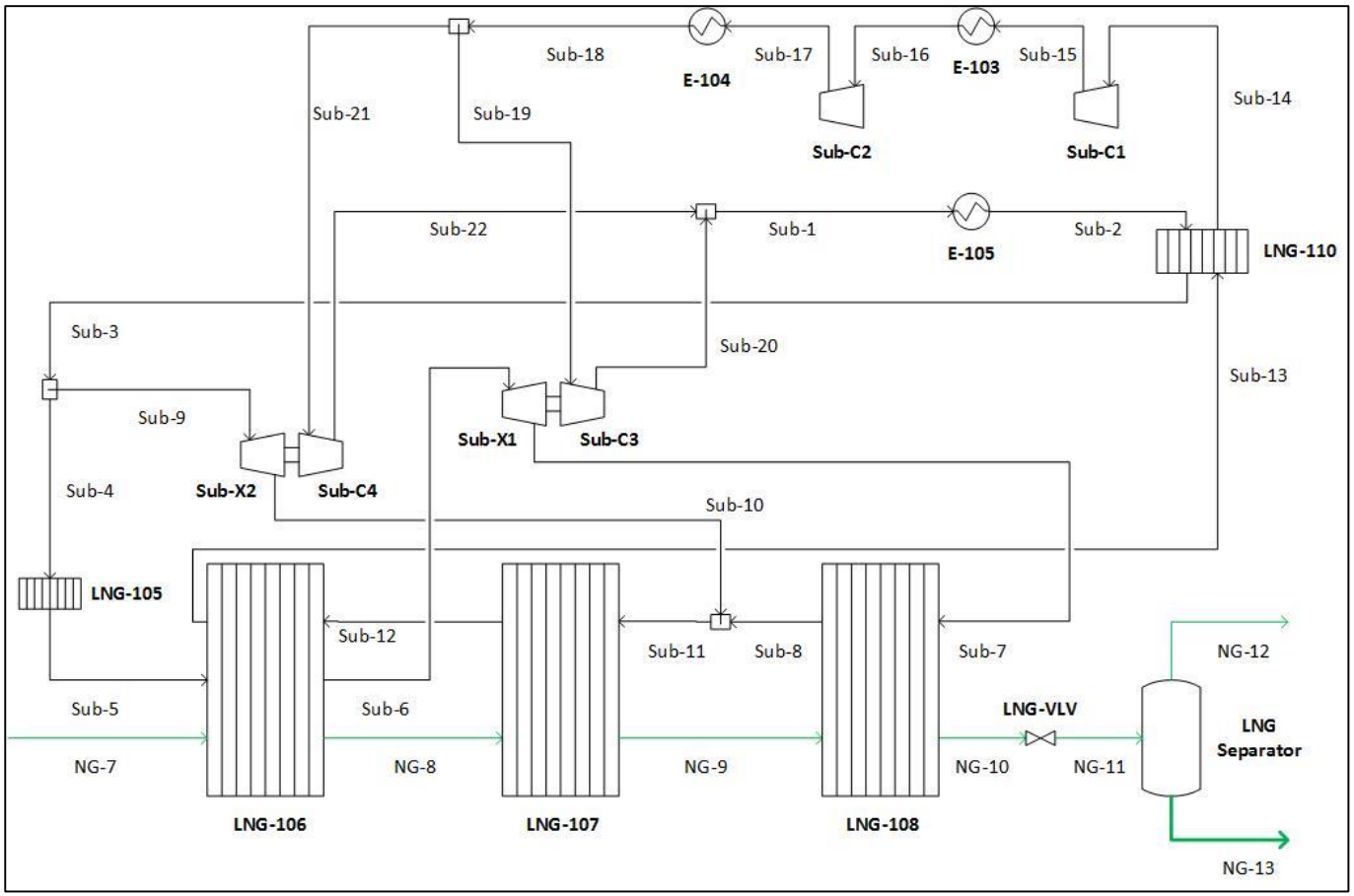

Figure 4- 3. Process flow diagram of the sub-cooling section.

4.11. Results and discussion

The simulation results can be summarized as Table 4-3 and Table 4-4. The proposed cycle shows enhanced efficiency than existing turbine-based processes with specific power comparable to mixed refrigerant processes.[78] It is difficult to compare liquefaction processes precisely based on specific power since the conditions are not standardized for different papers. The specific power of liquefaction process can vary due to many conditions including feed gas composition, feed gas pressure, temperature of cooling water in heat exchangers, pressure drop in heat exchangers, adiabatic efficiency of turbo machinery, etc.

Specific power of the developed N2O-N2O-N2 cascade cycle was 1138 kJ/kg. Efficiency of other liquefaction processes is shown in Table 4-4. It is notable that the efficiency (specific power) is considerably lower than single and double nitrogen cycle. It is comparable to mixed refrigerant cycles and cascade processes. So it can be concluded that natural gas liquefaction cycle with nonflammable refrigerants only was developed with similar power consumption compared to existing efficient cycles. N2O-N2O-N2 cascade cycle has potential advantages in practice due to simplicity and reliability of single-component refrigerant system.

Table 4- 3. Results of the N2O-N2O-N2 process.

Variable	Value	Dimension
Natural gas feed flow rate	228.0	[ton/h]
LNG production	206.9	[ton/h]
Pre-cooling section		
N2O flow rate	885.5	[ton/h]
N2O compressor duty	17.99	[MW]
Condensation section		
N2O flow rate	271.4	[ton/h]
N2O compressor duty	6.38	[MW]
Sub-cooling section		
N2 flow rate	1159	[ton/h]
N2 compressor duty	53.60	[MW]
N2 expander duty	12.55	[MW]
N2 net compressor duty	41.05	[MW]

Table 4- 4. Specific power of the N2O-N2O-N2 process.

Variable	Value	Dimension
LNG production	206.9	[ton/h]
Total compressor duty	65.42	[MW]
Specific power	316.2	[kWh/ton]
	13.18	[kW/t/d]
	1138	[kJ/kg]

Table 4- 5. Specific power of other liquefaction processes. [78]

Process	C3MR	Cascade	DMR	SMR	Single N2	Double N2
Specific power (kJ/kg)	1054	1218	1080	1253	3266	1426

4.12. Case study with a leaner feed gas

The specific power of the liquefaction process varies with change in feed natural gas composition. Leaner feed gas with higher fraction of lighter hydrocarbons will give a lower condensing temperature with decreased boiling point and thus decrease the process efficiency. On the other hand, richer feed gas with higher fraction of heavier hydrocarbons will increase the process efficiency. A case study for feed gas with composition in Table 4-6 was performed. The results are summarized in Table 4-7. Feed gas pressure and mass flow rate and final LNG temperature specification (-155℃) was remained same as the original case. Note that LNG production rate decreased from 206.9 ton/h to 205.9 ton/h. Also overall power consumption increased from 65.42 MW to 69.38 MW. For a very lean gas, it might not condense at -78.6℃. In this case, the expansion pressure of N2O in condensing section must be lower than 1.5 bar.

Table 4- 6. Composition of natural gas feed for lean gas case study

Component	Mole Fraction
Nitrogen	0.040
Methane	0.910
Ethane	0.040
Propane	0.010
i-Butane	0.000
n-Butane	0.000
i-Pentane	0.000

Table 4- 7. Results of the lean gas case study.

Variable	Value	Dimension
Natural gas feed flow rate	228.0	[ton/h]
LNG production	205.9	[ton/h]
Pre-cooling section		
N2O flow rate	868.9	[ton/h]
N2O compressor duty	17.64	[MW]
Condensation section		
N2O flow rate	267.0	[ton/h]
N2O compressor duty	6.73	[MW]
Sub-cooling section		
N2 flow rate	1274	[ton/h]
N2 compressor duty	58.92	[MW]
N2 expander duty	13.90	[MW]
N2 net compressor duty	44.02	[MW]

CHAPTER 5 : Retrofit design of liquefied natural gas regasification process* [79]

5.13. Introduction

Recently, LNG receiving terminals have been constructed worldwide due to a continuous increase in LNG demand. LNG receiving terminal has the role of transporting the LNG from the carrier and supplying it to industrial or residential customers. Imported LNG is stored in its liquid state in storage tanks at the LNG receiving terminal. In order to deliver LNG to the customer, LNG is vaporized through a regasification process. [80] Vapor continuously evaporates from LNG since LNG absorbs the heat in the storage tank and in the cryogenic pipelines during unloading and storage. This vapor is called boil-off gas (BOG). It causes safety problems in the LNG facilities since the pressure inside that facility increases with the generated BOG. Over-treatment of the BOG consumes excess energy. Hence, proper handling of BOG is required for an optimal design of a LNG receiving terminal.[81]

Usual BOG handling methods for LNG receiving terminals are recondensation and direct compression. The recondensation method is shown in Figure 5-1. BOG is compressed to around 10 bar through a BOG compressor and mixed with enough send-out LNG, which is pumped at same pressure in the recondenser so to obtain a liquid mixture. The LNG mixed with the BOG is compressed to pipeline pressure in

* The partial part of this chapter is taken from the author's published paper in the journal.[79]

high-pressure (HP) pump and vaporized by seawater. The direct compression method is shown in Figure 5-1. The BOG in a storage tank is compressed to the pipeline pressure through more than 2 compression stages and then, transported to the pipeline with the send-out natural gas.[82] Generally, the direct compression method has higher operating costs than the recondensation method because the gas is directly compressed to a high pressure. Most LNG receiving terminals, which include the Incheon LNG receiving terminal in Korea, use a combined method of recondensation and direct compression.[83] As shown in Figure 5-1, the compressed BOG from the BOG compressor is condensed by mixing with the LNG in the recondenser. If the send-out flow rate of the LNG from the storage tank is insufficient to condense all of the BOG, BOG that cannot be condensed accumulates in the recondenser. Thereupon, the remaining BOG in the recondenser is compressed to the pipeline pressure through the HP compressor and is directly transported to the pipeline mixed with the natural gas.[80] Since the operation of the HP compressor requires considerable energy and hence, has considerable operating costs, it is desirable to minimize the operation of the HP compressor. In the BOG handling process, high-pressure LNG compressed by HP pump has a useful cryogenic energy. The high-pressure LNG stream, which is maintained around -120℃, should be heated so it can be vaporized at 0℃ with the seawater vaporizer. Hence, the cryogenic energy of this high-pressure LNG stream can be used to improve the BOG handling process.

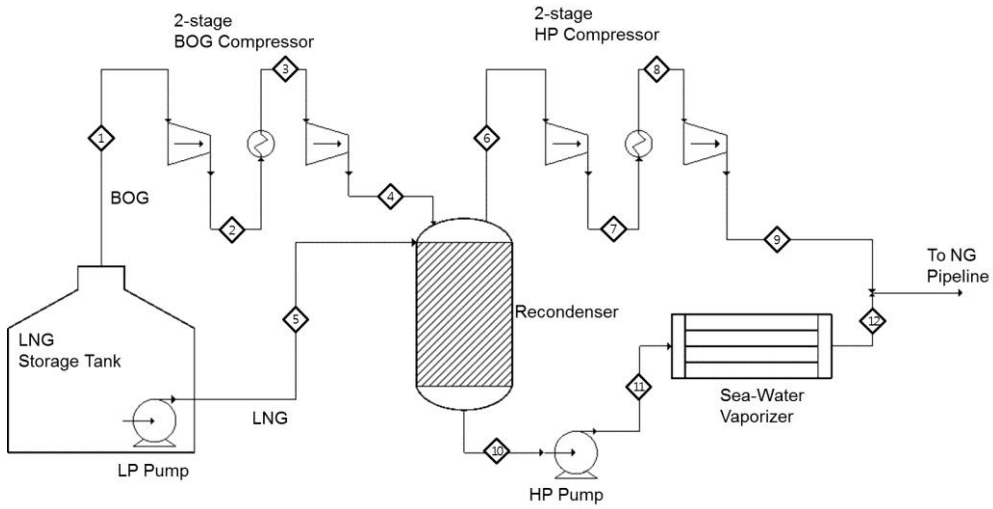

Figure 5- 1. Process flow diagram of the BOG handling process in LNG receiving terminal.

Recently, research on the LNG receiving terminals is usually focused on analyzing the operation of a specific facility in the LNG receiving terminal and the utilization of the cryogenic energy of the LNG stream. Lee et al. suggested a reliable unloading operation procedure for a mixed operation of above-ground and in-ground storage tank.[84] Kim et al. analyzed mixing drums and heat exchangers as a BOG recondenser.[85] Lim et al. developed the methodology for a stable simulation of the LNG pipe.[86] Studies on the operation of the BOG compressor at the Pyeoungtaek LNG receiving terminal was performed with industrial data. [81] [87] Liu et al. optimized a process for the multi-stage recondensation of the BOG based on a thermodynamic analysis.[88] Studies on optimal operating conditions for a regasification facility have been performed.[89] [90] Various studies have been proposed a power generation plant using cryogenic energy applied to power cycle. Liu and You developed the mathematical model to predict the total heat exergy of LNG.[91] Qiang et al. analyzed the power cycle based on the cold energy of LNG.[92] Also Qiang et al. carried out the exergy analysis for several power cycles used for recovering the LNG cold energy.[93] Sun et al. proposed and analyzed the cryogenic thermo-electric generator.[94] Kim and Hong analyzed the exergy of current LNG receiving terminal and cold power generation plant.[95] Szargut and Szczygiel proposed and optimized power plant using LNG cryogenic exergy.[96] A cogeneration plant using the BOG and cryogenic energy has been suggested.[97]

Based on a literature survey, few studies on the retrofit design of the BOG handling process has been reported in term of reducing the operating energy. The improvement and optimization of the BOG handling process have the potential to reduce the operating costs of the natural gas facility.

The contribution of the study in this chapter is development of the retrofit design of a BOG handling process in which the design variables are optimized for total cost minimization. Cryogenic energy of the LNG is used to directly reduce the capital cost and operating cost without additional power generator. In this paper, we used the retrofit method which includes the thermodynamic analysis, process simulation and optimization. This study describes a general operating line of a BOG handling process based on thermodynamic analysis. In the operating line, the opportunity of design improvement and the reasons of energy saving are described by comparing with base case design and retrofit design. Based on the thermodynamic analysis, a superstructure of the retrofit design is developed and the design variables, which are in direct relationship with capital cost and operating cost, are defined. Since the objective function of optimization problem is calculated using process simulation results, the optimization algorithm of the design variables is based on process simulation. The optimal values of design variables are achieved using SQP (Sequential Quadratic Programming) solver in MATLAB® . Finally optimal design of the retrofit BOG handing process is verified through the sensitivity analysis of external operating conditions.

5.14. Methodology

The algorithm of the retrofit method is shown Figure 5-2 in which it aims to minimize the capital cost and operating cost of BOG handling process. Retrofit procedure starts with thermodynamic analysis of BOG handling process. The P-H (pressure-enthalpy) diagram is generated from LNG properties based on Peng-Robinson equation of state. As the operating line of the BOG handling process is presented in P-H diagram, the possibility for improvement of the BOG handling process is investigated. The retrofit opportunity for efficient design is obtained from a result of the thermodynamic analysis for the operating line. In the next step, the superstructure of the retrofit design is developed by applying the retrofit opportunity based on thermodynamic analysis. To obtain the optimal design, the optimization problem of retrofit design is formulated, in which the main objective is the minimization of capital cost and operating cost. The design variables, which affect the capital cost and operating cost, are defined to formulate the objective function based on the superstructure of the retrofit design. In addition, design constraints of the optimization problem are determined using the process simulation of the superstructure.

Since the optimization problem of retrofit design is nonlinearly constrained problem, it is solved using sequential quadratic programming (SQP) method. At each iteration step, the optimization problem is approximated by quadratic form. Then the quadratic programming subproblem is solved using a combination of active-set strategy and process simulation of retrofit design to calculate the Lagrange multiplier and search direction for next iteration. If the termination criteria of QP solution are met, design variables at current iteration step (x^k) are optimal values of the SQP problem and the solver stops. Otherwise, the step length for next iteration is evaluated using line

search method. Then, x^k is updated by search direction and step length to generate new value x^{k+1}. In the next iteration, the updated values are used for the next step. In this paper, the process simulation of the retrofit design was conducted by Aspen Plus® and the SQP was solved by MATLAB® .

After the optimal design values of retrofit process are obtained by solving the SQP, sensitivity analysis for the design parameters which have variability, such as LNG demand rate, is performed to verify the profitability of the retrofit design. Finally the retrofit design is proposed after verification of the profitability.

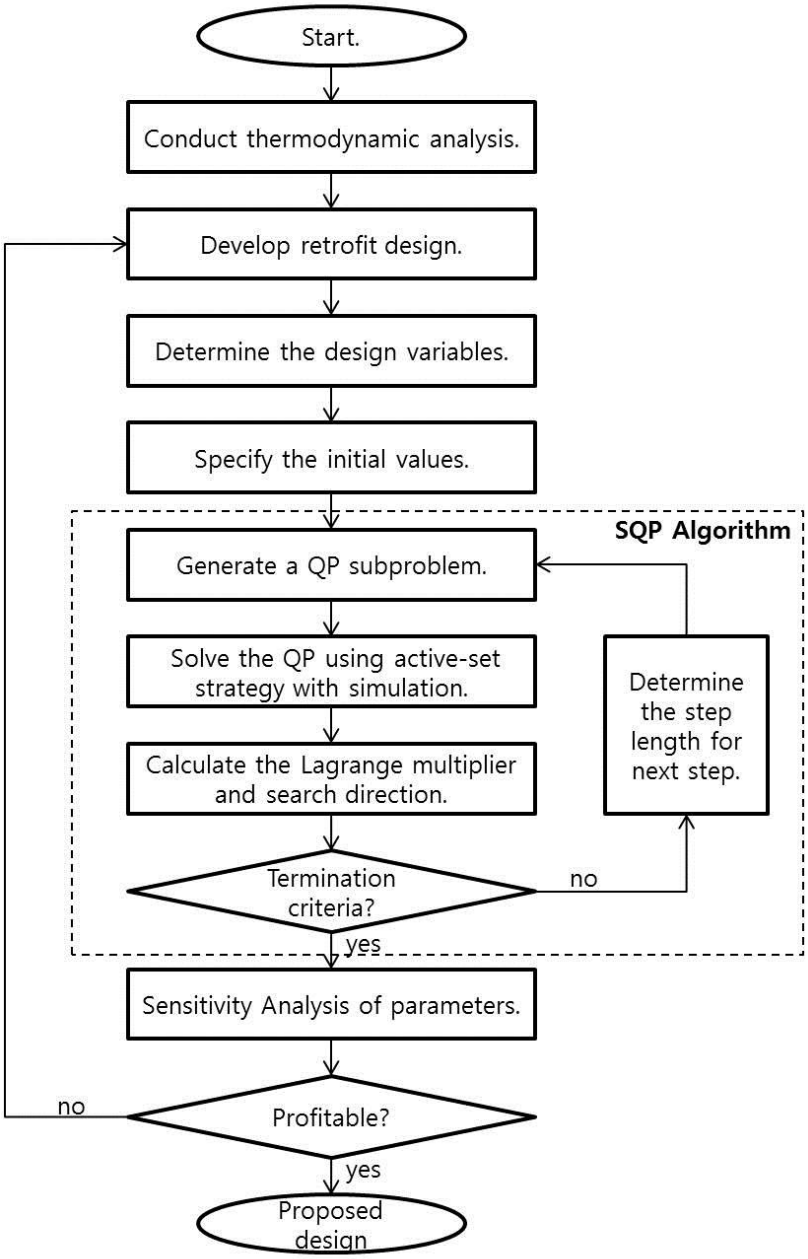

Figure 5- 2. Algorithm proposed for retrofit design.

5.15. Case study

5.15.19. Base case design definition

Various studies on the practical operation which include the BOG compressor were conducted about the Pyeongtaek LNG receiving terminal. The practical operations of the compressor [81] [87] and the recondenser [85] [98], operator's feedback [99] [100] , basic design information[101] of the Pyeongtaek LNG receiving terminal were indicated. In this study, base case design of the BOG handling process was determined based on the practical design conditions of the Pyeongtaek LNG receiving terminal. Details of the base case design are presented in Table 5-1. However, the base case design is not identical to Pyeongtaek LNG receiving terminal due to only one difference, the HP compressor. Most BOG handling processes use HP compressors for BOG handling while Pyeongtaek LNG terminal utilizes BOG as fuel since it is adjacent to other plants. HP compressor in Pyeongtaek LNG terminal is replaced with flare stack and power plant.[98] Base case design was determined assuming that the HP compressor is used for the BOG handling. Therefore the process flow diagram of the base case design is identical to Figure 5-1 and design conditions are based on Pyeongtaek LNG receiving terminal in Table 5-1.

Table 5- 1. The design conditions of the base case design.

Parameter	Value
Storage tank pressure, mbarg	170
Suction temperature of BOG compressor, ℃	-120
Temperature of LNG before recondensation, ℃	-155
BOG flow rate, ton/h	30
Minimum LNG send-out rate, ton/h	200
Recondensation pressure, kg/cm^2	10
Send-out pressure. kg/cm^2	76
Send-out temperature, ℃	0

The BOG compressor and HP compressor consisted of a 2-stage compression in which the pressure ratio is identical.[99] The generation rate of the BOG in the storage tanks was determined by a normal operation case[81] and the send-out rate of the LNG were determined by a minimum send-out case.[99] Since this paper proposes an advanced process design, we choose the minimum send-out case, which has difficulties in handling the BOG. For the above reason, a retrofit design based on the minimum send-out case can easily handle BOG using recondensation whenever the send-out rate of the LNG changes. Modeling and simulation of the base case was conducted in Aspen Plus® in order to calculate the total operating cost of the BOG handling process. The stream data of the process simulation is presented in Table 5-2. Stream numbers in Table 5-2 correspond with the stream number in Fig 5-1. Temperature values of the compressor inter-streams, stream 2 and 7, are at -49.6 ℃ and -58.1 ℃, respectively and there is no need to inter-cool these streams. Therefore, stream 3 and 8 are identical to stream 2 and 7. Operating costs of each unit in the base case are presented in Table 5-3. The operating costs of the whole process considered 5 units, which included the BOG compressor, LP pump, HP compressor, HP pump, and seawater pump.

Table 5- 2. Stream data of the base case design.

	1	2	4	5	6	7	9	10	11	12
Temperature, ℃	-120	-49.6	46.8	-155.0	-122.6	-58.1	29.8	-122.6	-117.7	0.00
Pressure,bar	1.12	3.43	9.81	13.73	9.81	27.02	74.53	9.81	74.53	74.53
Vapor fraction	1	1	1	0	1	1	1	0	0	1
Mass flow, t/h	30.0	30.0	30.0	200.0	4.7	4.7	4.7	225.3	225.3	225.3

Table 5- 3. Operating costs of the base design.

Unit	Energy costs
1st stage BOG compressor, kW	1189.91
2nd stage BOG compressor, kW	1699.19
1st stage HP compressor, kW	144.81
2nd stage HP compressor, kW	209.94
HP pump, kW	1279.92
LP pump, kW	188.39
SW Pump, kW	49.07
Sum, kW	4761.24

The BOG flow rate, which is difficult variable to measure, is sharply fluctuated in the LNG receiving terminal. To analyze effects of a shift in the BOG flow rate on the result of simulation, the total operating costs of the process model are computed changing ±10% of the BOG flow rate as shown in Figure 5-3. If the BOG flow rate is changed in the range of ±10%, the result of process model is changed in the range between -13.4% and 14.8%. Thus, the result of process model is greatly affected by BOG flow rate. It is necessary to use the accurate value of BOG flow rate for process simulation in this method.

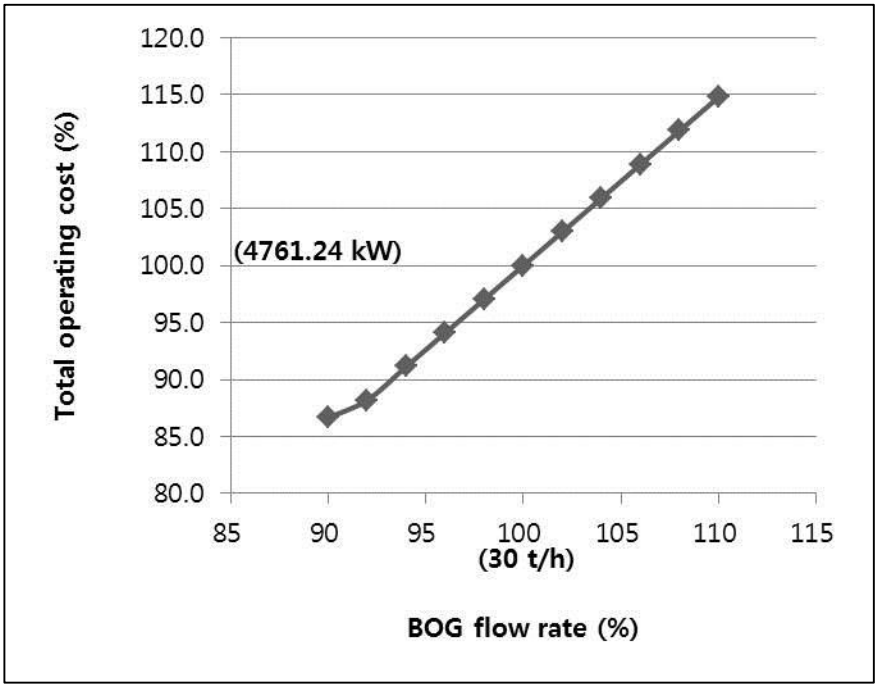

Figure 5- 3. Total operating cost with varying BOG flow rate.

5.15.20. Thermodynamic analysis of the base case design

A P-H diagram of the base design is shown in Figure 5-4 to analyze operations in the BOG handling process. The pressure axis in Figure 5-4 is the logarithmic coordinate. The blue line is the isothermal line, which presents the operation state at a specific temperature. The red line is the bubble point and dew point, which yield information on the phase change. The green line is the isentropic line of operation; LNG or BOG is compressed following the isentropic line through the pump and compressor. When the LNG or BOG moves following the isentropic line, the magnitude of the x-axis denotes the operation cost of the related unit. Points 1 and 2 represent the state of the LNG and BOG in the storage tank. LNG is pressurized to the recondensation pressure with the LP pump at point 3. The BOG is compressed to the recondensation pressure with the BOG compressor (point 4). Although operation of the BOG and HP compressor is shown as 1 path in the P-H diagram, the BOG and HP compressor consist of 2 stages. In the recondenser, the LNG and BOG are mixed at the recondensation pressure to form a liquid mixture, which becomes saturated LNG (point 5). The liquid mixture from the recondenser is pressurized to the send-out pressure with the HP pump (point 6). The LNG stream at high pressure is heated by seawater so to transport it in the vapor state. However, the BOG, which cannot be condensed in the recondenser, goes through the HP compressor to be directly compressed to the send-out pressure and supplied to the customer mixed with the send-out natural gas (point 7).

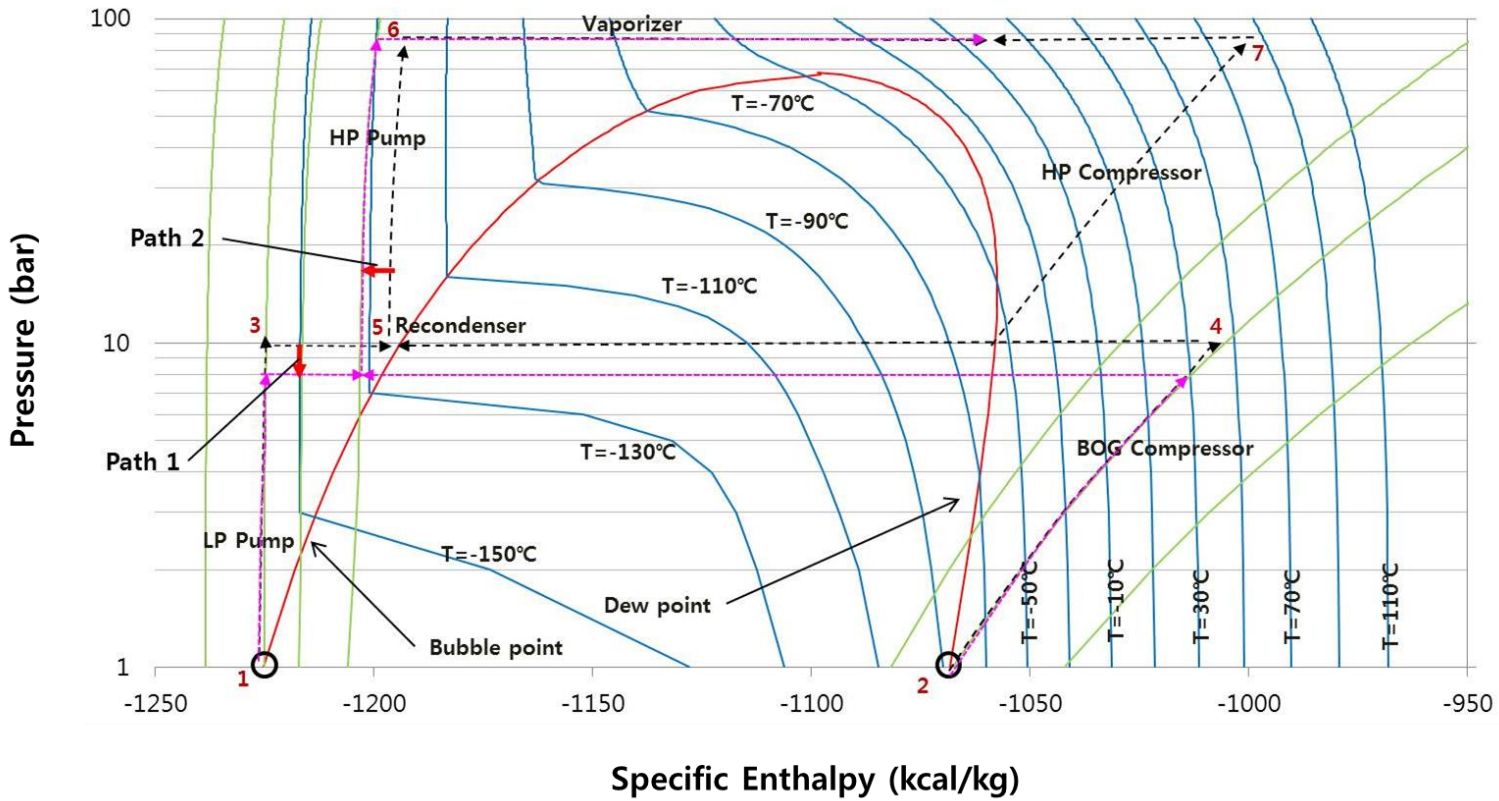

Figure 5- 4. Pressure-enthalpy diagram of the BOG handling process.

5.15.21. Proposal of the retrofitting design for energy saving

If the BOG from the BOG compressor is cooled with a heat exchanger using the high-pressure LNG stream (point 6 in Figure 5-4), the operating lines of the BOG handling process in the P-H diagram changes as following path 1, 2 in Figure 5-4. Since the temperature of the liquid mixture is lower through the path 1, 2, the recondensation pressure can be lower; a decrease in the recondensation pressure reduces the operating cost of the BOG compressor. In addition, a larger BOG flow rate can be condensed to reduce the operating cost of the HP compressor. The scheme of this design is shown in Figure 5-5. A high-pressure LNG stream goes through the BOG cooler to cool down the BOG stream. This method provides a lower operating pressure in the recondenser and a larger BOG rate to be condensed. It can reduce the operating energy of the BOG and HP compressors.

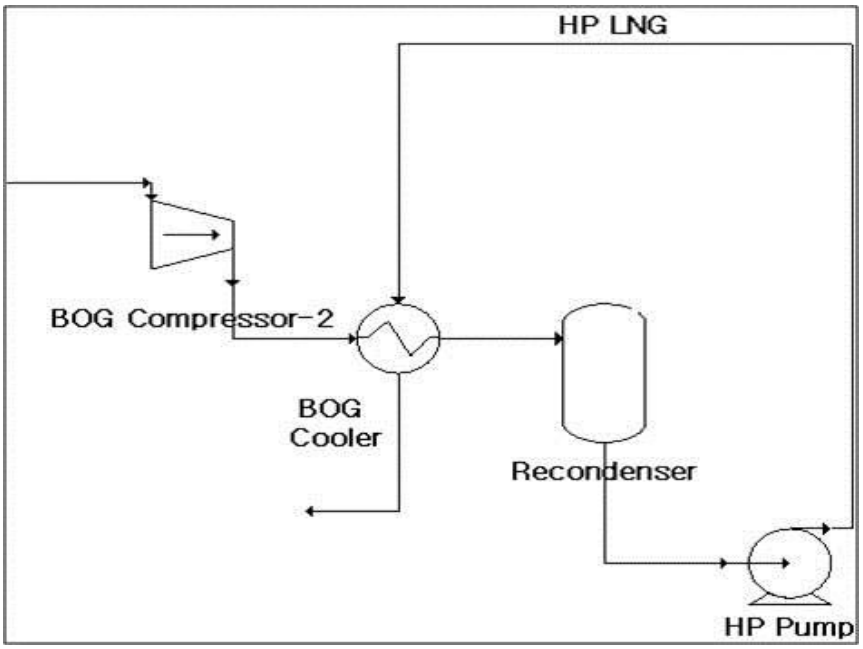

Figure 5- 5. A scheme of the BOG handling process with the BOG cooler.

The BOG and HP compressors usually consist of 2 stages due to a compression ratio of 7~10. Hence, the cryogenic energy of the high-pressure LNG stream is utilized for intercooling in the compressors. This method improves the efficiency of the compressors decreasing the temperature of the BOG inter-stream. As shown in Figure 5-6, the operation paths of the compressors shift to paths that are more efficient. In the proposed paths, the operating costs of the BOG and HP compressors are reduced. The high-pressure LNG stream is utilized for intercooling in the compressors by the compressor intercoolers in Figure 5-1.

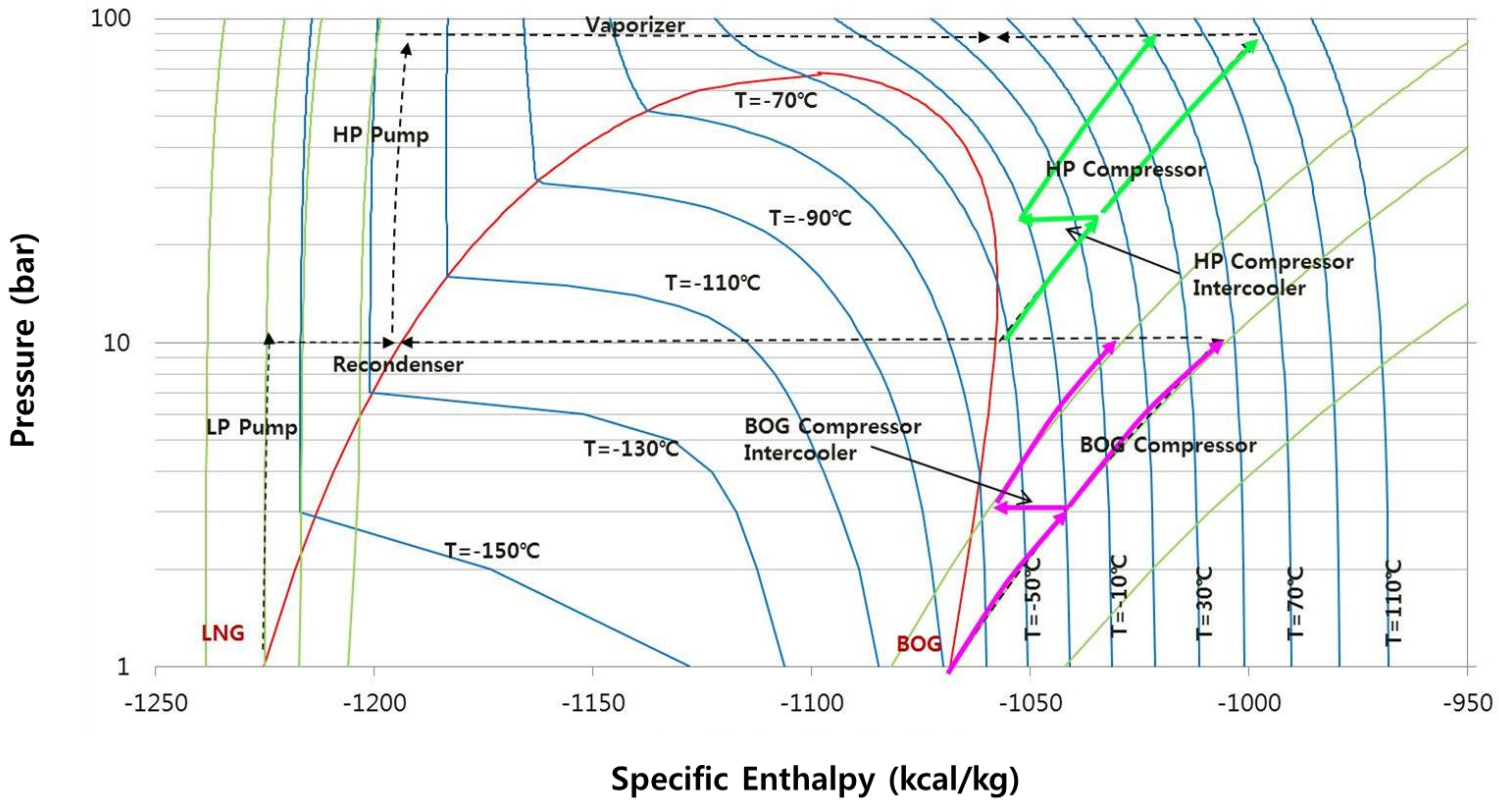

Figure 5- 6. Pressure-enthalpy diagram of the BOG handling process with the intercooler of the BOG and HP compressors.

The superstructure of the retrofit design was based on the above thermodynamic analysis of the BOG handling operation. As shown in Figure 5-7, the high-pressure LNG stream from the HP pump splits into 3 streams. Each stream flows through the BOG compressor intercooler, the BOG cooler, and the HP compressor intercooler to cool down the BOG stream; thereby, the operating costs of the BOG and HP compressors are reduced. After the 3 branch streams pass through the heat exchangers, these streams combine to become one stream. This single LNG stream then moves to the seawater vaporizer. The retrofit design provides a lower recondensation pressure and a larger condensing rate for the BOG and improves the compressor efficiency for energy savings.

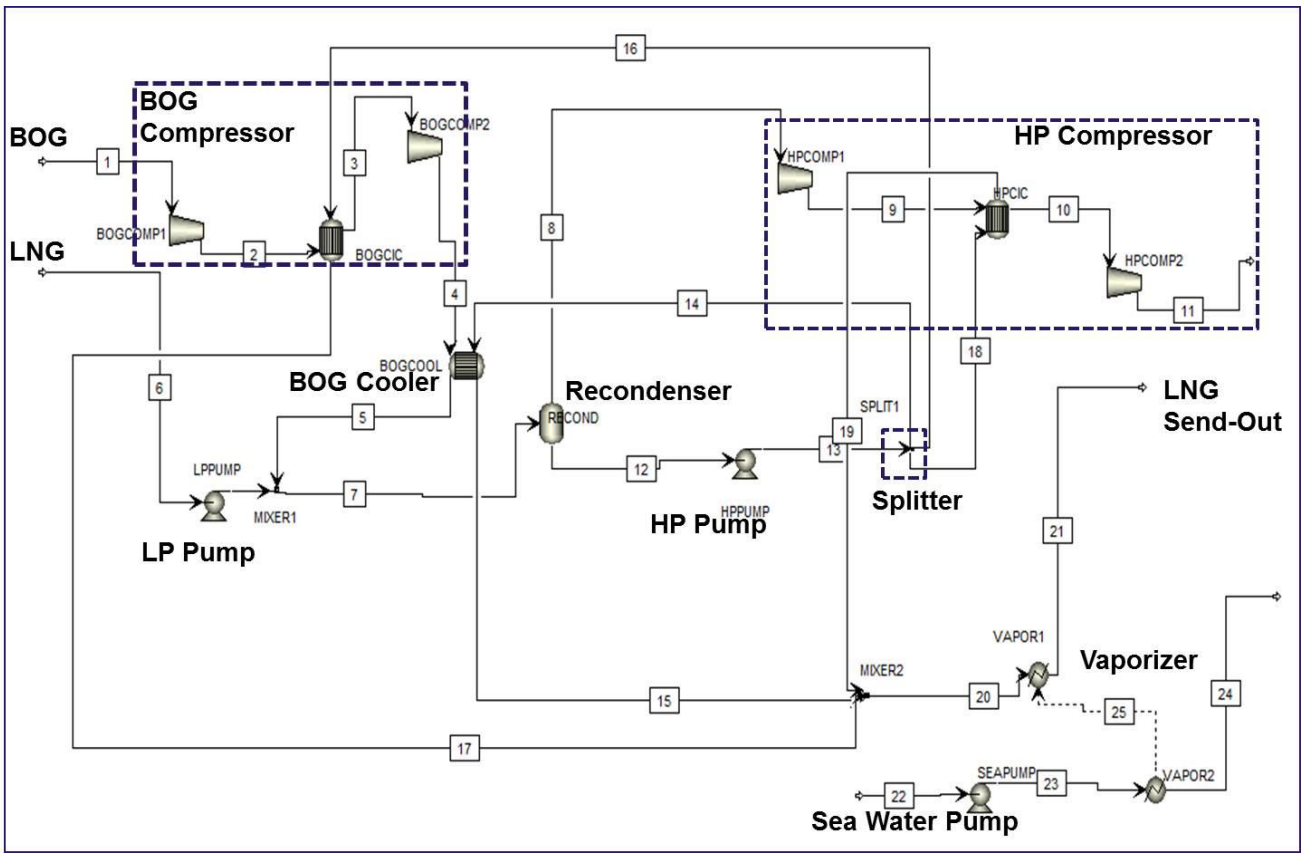

Figure 5- 7. The superstructure of the retrofit design.

5.15.22. Optimization of design variables

The design variables of the proposed superstructure need to be optimized to minimize the total operating cost. [82] [88] [102] For this purpose, modeling of the proposed superstructure was done with Aspen Plus® . Optimal design and operating variables were obtained with specified constraints to minimize the operating costs. The objective function of this optimization problem was to maximize the venture profit (VP), which measures the profitability of the design for the BOG handling process shown by Eq. (5-1). The return on investment is 0.2. The saving costs (C_S) are obtained to calculate the multiplication of the price of electricity (P_e) and the difference between the operating cost of the base design and the proposed design shown by Eq. (5-2). The capital cost of the retrofit design considers the equipment cost of the additional heat exchanger; the equipment cost of the heat exchanger was calculated by referring to Warren Seider.[103] The purchase cost (C_P) of the heat exchanger is calculated by multiplication of the pressure factor (F_P), the material factor (F_M), the tube-length factor (F_L) and base purchase cost (C_B) shown in Eq. (5-3). The base purchase costs are correlated in terms of heat-exchanger surface areas (A_i), which are calculated by process simulation, in ft^2 shown in Eq. (5-4). The material factor is a function of surface area shown in Eq. (5-5). The parameters a and b are 2.70 and 0.07, respectively, since stainless steel is used as the material of the shell and tube side. The tube-length factor is 1.25 for tube length below 8 feet. The pressure factor is based on the shell-side pressure (P) in psig shown in Eq. (5-6).

$$\mathrm{VP} = C_S - i_{min} C_P \tag{5-1}$$

$$C_S = \left(\sum W_{Basic} - \sum W_{Proposed} \right) \times P_e \tag{5-2}$$

$$C_P = F_P F_M F_L C_B \tag{5-3}$$

$$C_B = exp\left\{ 11.147 - 0.9186 \left[\ln \left(A_i \right) \right] + 0.09790 \left[\ln \left(A_i \right) \right]^2 \right\} \tag{5-4}$$

$$F_M = a + \left(\frac{A_i}{100} \right)^b \tag{5-5}$$

$$F_P = 0.9803 + 0.018 \left(\frac{P}{100} \right) + 0.0017 \left(\frac{P}{100} \right)^2 \tag{5-6}$$

5.15.23. Design variables

In this optimization problem, design variables were divided into 4 types. As shown in Figure 5-8, the first design variable was the recondensation pressure (P_R) at which the BOG stream from the BOG compressor and LNG stream from the LP pump is mixed to condense the BOG. If the recondensation pressure is raised, the operating cost of the HP compressor is reduced due to the additional condensation of the BOG. However, the operating cost of the BOG compressor and the LP pump increases as the discharge pressure of the BOG compressor and LP pump increases. Hence, it is necessary to find the optimal recondensation pressure to minimize the operating cost.

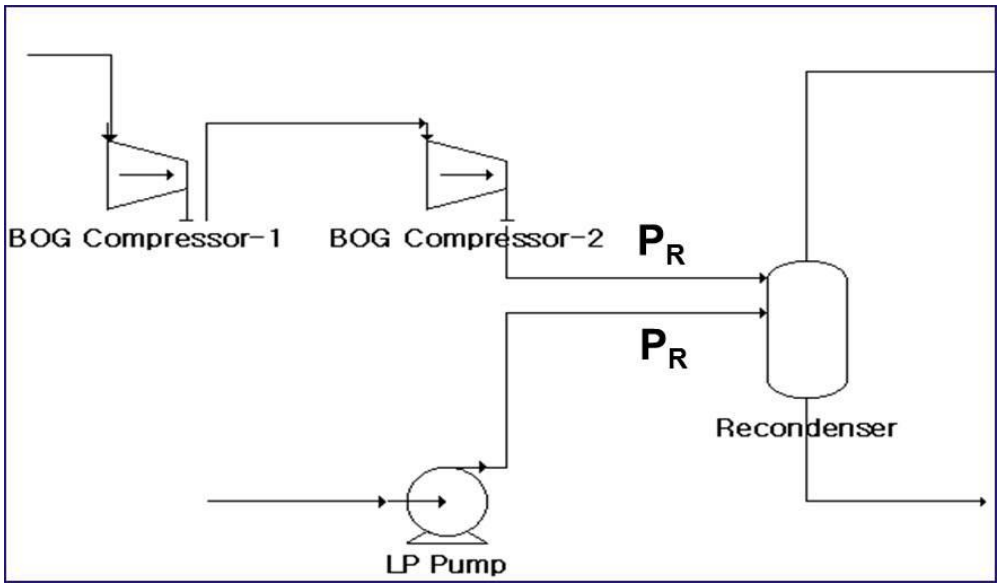

Figure 5- 8. The recondensation pressure.

The second design variable was the heat transfer area of the heat exchangers that are added to the proposed design. The heat transfer areas of the BOG cooler (A_1) in Figure 5-5, the intercooler of the BOG compressor (A_2) and the intercooler of the HP compressor (A_3) in Figure 5-1 need to be determined for an optimal retrofit design. If the heat transfer areas increase, the effects of cooling the BOG consistently increase along with the capital cost of the heat exchangers. For this reason, the optimal heat transfer area of each heat exchanger needs to be determined to maximize the VP. The third design variable was the compression ratio (r_{Bi}, r_{Hi}) for each stage of the BOG and HP compressors. The total compression ratio of the compressors is determined by the recondensation pressure, but the compression ratio for each stage should be determined to achieve minimum operating costs. In the proposed design, the high-pressure LNG stream is used for the 3 heat exchangers. The high-pressure LNG stream splits into 3 paths. The fourth design variable was the split ratio of the high-pressure LNG stream to the BOG cooler (s_1), the BOG compressor intercooler (s_2), and the HP compressor intercooler (s_3) shown in Figure 5-9. For a minimum total operating cost, the split ratio needs to be optimized.

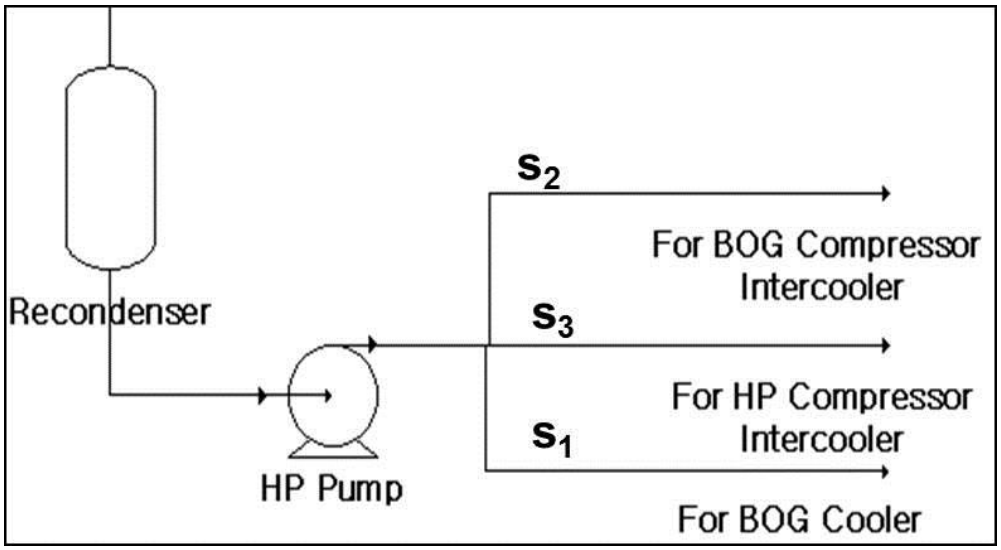

Figure 5- 9. The split ratio of the high-pressure LNG stream to the BOG cooler (S1), the BOG compressor intercooler (S2) and the HP compressor intercooler (S3).

The constraints were considered for the feasible design variables, which were obtained by solving the optimization. Constraints on heat and mass balance, on a theoretical model for unit operation, and on phase equilibrium were taken into account using process modeling. The compression ratio of each stage should change in the range from 1.5 to 3.5 shown by Eq. (5-7) and (5-8). In addition, the discharge pressure of the BOG compressor should the same the recondensation pressure, which was already determined, and the discharge pressure of the HP compressor should be 76 kg/cm^2 of the send-out pressure shown by Eq. (5-9) and (5-10).

The split of the high-pressure stream should remain in the range from 0 to 1 shown by Eq. (5-11). The summation of the split ratio should become one shown by Eq. (5-12). When the BOG stream moves to the second stage of the compressors, the phase of this stream should remain in the vapor state. The vapor fraction (vf_B, vf_H) of the BOG stream, which heads for the second stage of the compressors, should be maintained at one shown by Eq. (5-13) and (5-14). In addition, the temperature difference, which are correlated in terms of heat exchanger area, split ratio, heat capacity of BOG (C_{BOG}) and LNG (C_{LNG}), between the BOG stream and the high-pressure LNG stream in the BOG cooler (ΔT_1), in the BOG compressor intercooler (ΔT_2), and the HP compressor intercooler in (ΔT_3) should be higher than the minimum approach temperature (ΔT_{min}) shown by Eq. (5-15).

$$1.5 \le r_{Bi} \le 3.5, \quad i = 1, 2 \tag{5-7}$$

$$1.5 \le r_{Hi} \le 3.5, \quad i = 1, 2 \tag{5-8}$$

$$1.1 \times r_{B1} \times r_{B2} = P_R \tag{5-9}$$

$$P_R \times r_{H1} \times r_{H2} = 74.53 \tag{5-10}$$

$$0 \le s_i \le 1, \quad i = 1, 2, 3 \tag{5-11}$$

$$\sum s_i = 1, \quad i = 1, 2, 3 \tag{5-12}$$

$$vf_B(P_R, r_{B1}, A_2, s_2) = 1 \tag{5-13}$$

$$vf_H(P_R, r_{H1}, A_3, s_3) = 1 \tag{5-14}$$

$$\Delta T_i\left(A_i, s_i, C_{BOG}, C_{LNG}\right) \ge \Delta T_{min}, \quad i = 1, 2, 3 \tag{5-15}$$

5.16. Results and discussion

5.16.24. Comparison with the base design

The optimization problem formulated in Section 5.3 was solved with user defined non-linear programming in order to find the optimal design variables that can maximize the VP of the proposed design.

As presented in Table 5-4, a decrease in the recondensation pressure (from 9.81 bar to 5.56 bar) reduced the operating cost of the BOG compressor. Additionally in the proposed design, the BOG stream was totally condensed in the recondenser. Since there was no BOG rate for the HP compressor, the HP compressor was not put into operation, and the operating cost of the HP compressor became zero. Due to the above reason, the split ratio of the HP compressor intercooler and heat transfer area became zero in the optimization results. In this study, the proposed design was based on the minimum send-out case. If the BOG stream was totally condensed through the recondenser in the minimum send-out case in which the least amount of the LNG stream is used for the condensation, any case of the proposed design needs not to include the HP compressor. Thus, in the proposed design, the capital costs were reduced by eliminating the HP compressor unit, shown in Figure 5-10.

Table 5- 4. Comparison of the design variables.

Variable	Basic design	Proposed design
Recondensation pressure (PR), bar	9.81	5.56
Area of BOG cooler (A1), m^2	0	95.46
Area of BOG comp. intercooler (A2), m^2	0	96.70
Area of HP comp. intercooler (A3), m^2	0	-
Pressure ratio of BOG comp. (rB1)	2.86	2.00
Pressure ratio of BOG comp. (rB2)	2.86	2.35
Pressure ratio of HP comp. (rH1)	2.76	-
Pressure ratio of HP comp. (rH2)	2.76	-
Split ratio to BOG cooler (s1)	0	0.589
Split ratio to BOG comp. intercooler (s2)	0	0
Split ratio to HP Comp. intercooler (s3)	0	0.411

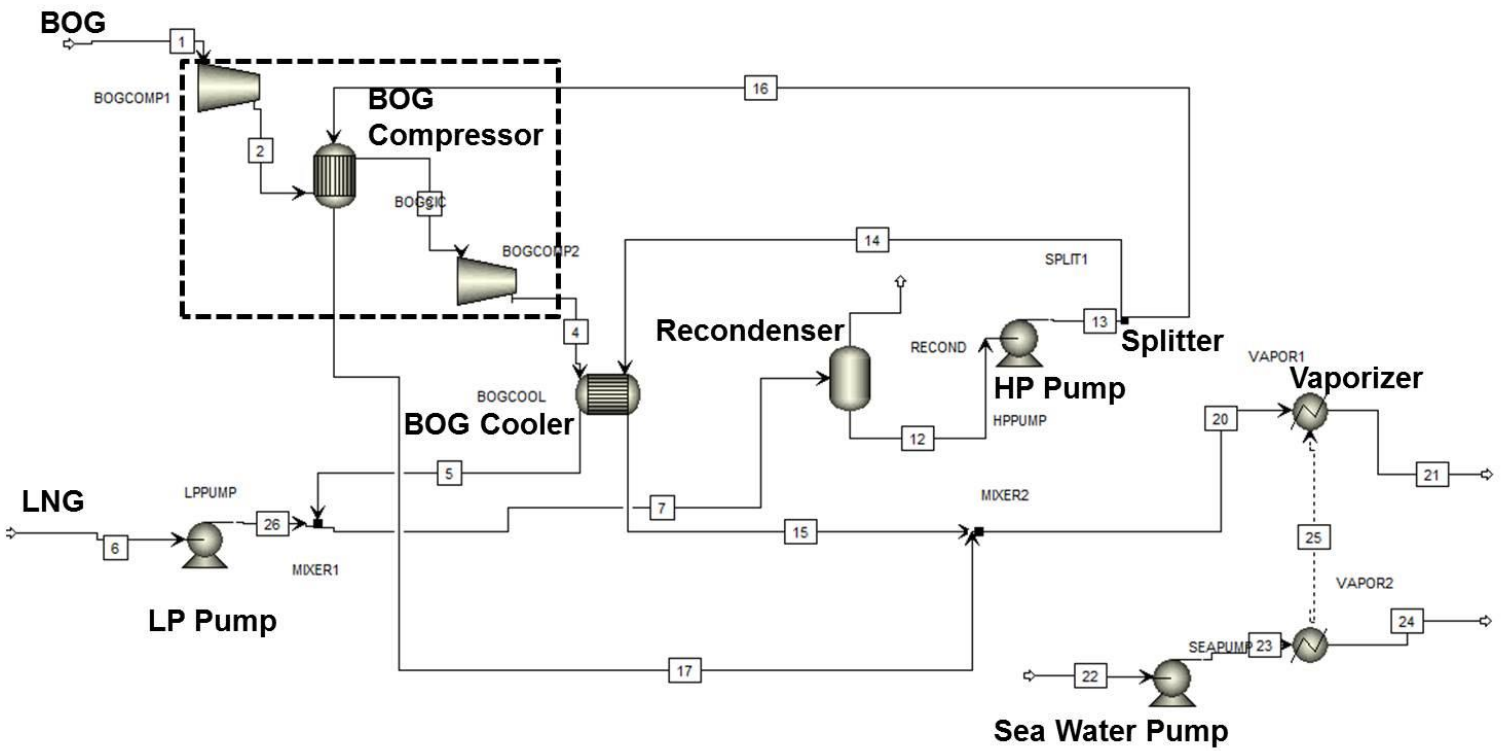

Figure 5- 10. The superstructure of the proposed design.

The operating costs of the base design and proposed design are shown in Figure 5-11. Due to the decrease in the recondensation pressure and increase in the compressor efficiency by intercooling, the operating cost of the BOG compressor was reduced. Since the BOG stream was totally condensed, the HP compressor was not put into operation and the operating cost of the HP compressor became zero. The proposed design totally reduced the energy cost of 36.84% in the minimum send-out case.

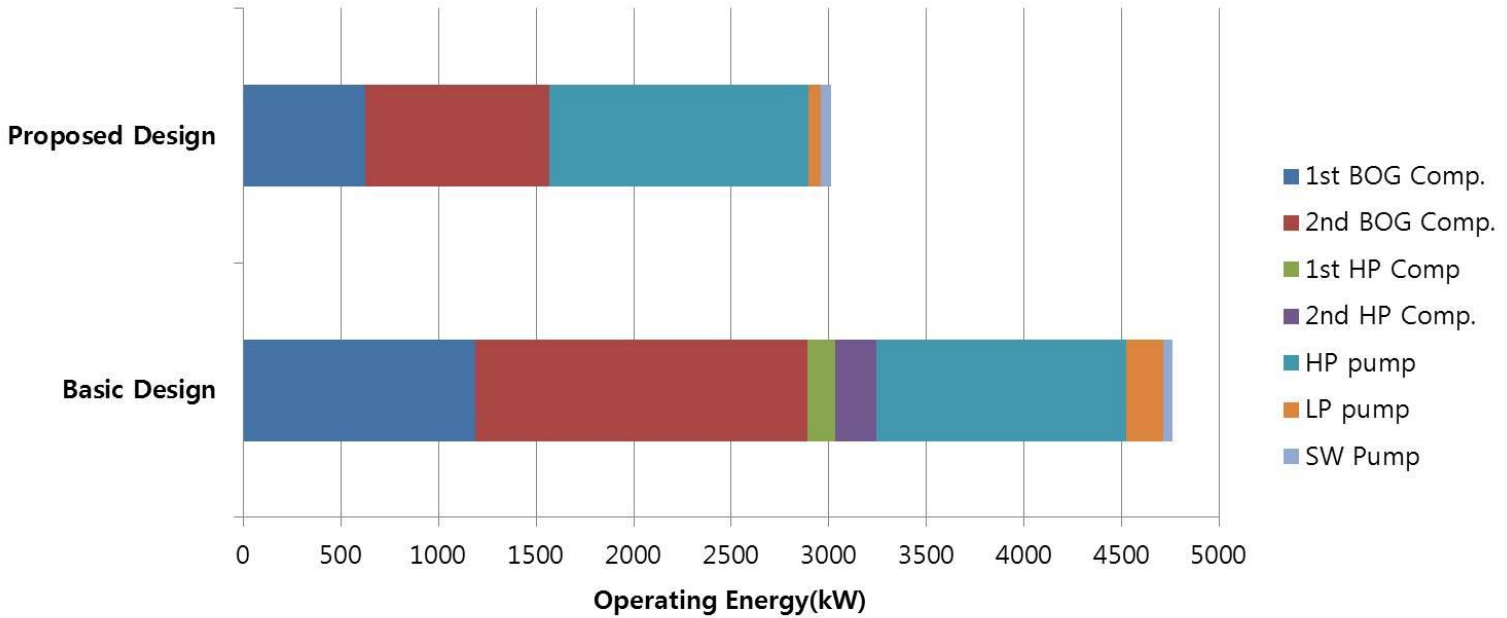

Figure 5- 11. A comparison of operating costs.

5.16.25. Sensitivity analysis

In order to find the effect of the LNG send-out rate, which changes due to changes in the seasons and time, the optimal LNG split ratio for the BOG cooler was determined by increasing LNG send-out rate from the minimum rate to the maximum rate.[101] Table 5-5 shows the operating costs as the split ratio for the BOG cooler and the LNG send-out rate change. At a send-out rate of 400,000kg/h, the operating costs due to the changing split ratio are shown in Figure 5-12.

Table 5- 5. Operating costs of the base design.

	Send-out flow rate (kg/h)	Split ratio(for BOG compressor intercooler)								
		0.1	0.2	0.3	0.4	0.5	0.6	0.7	0.8	0.9
Total operating cost (kW)	220,000	3,137	3,117	3,113	3,111	3,111	3,111	3,112	3,112	3,116
	240,000	3,240	3,222	3,219	3,217	3,217	3,217	3,218	3,218	3,221
	260,000	3,346	3,330	3,326	3,325	3,325	3,325	3,326	3,326	3,329
	280,000	3,453	3,439	3,436	3,435	3,435	3,435	3,435	3,435	3,437
	300,000	3,562	3,548	3,546	3,545	3,545	3,545	3,545	3,545	3,547
	320,000	3,671	3,659	3,656	3,656	3,656	3,656	3,656	3,657	3,658
	340,000	3,781	3,770	3,767	3,767	3,767	3,767	3,768	3,768	3,770
	360,000	3,892	3,881	3,879	3,879	3,879	3,879	3,880	3,881	3,882
	380,000	4,003	3,994	3,992	3,991	3,992	3,992	3,992	3,993	3,995
	400,000	4,115	4,106	4,104	4,104	4,105	4,105	4,105	4,106	4,108

Table 5-5. (continued)

	Send-out flow rate (kg/h)	Split ratio(for BOG compressor intercooler)								
		0.1	0.2	0.3	0.4	0.5	0.6	0.7	0.8	0.9
Total operating cost (kW)	600,000	5,256	5,251	5,251	5,251	5,251	5,252	5,252	5,254	5,257
	800,000	6,417	6,413	6,413	6,414	6,414	6,414	6,415	6,416	6,419
	1,000,000	7,584	7,582	7,582	7,583	7,583	7,583	7,584	7,585	7,588
	1,200,000	8,756	8,755	8,755	8,755	8,755	8,756	8,756	8,757	8,760
	1,400,000	9,930	9,929	9,929	9,929	9,930	9,930	9,930	9,931	9,934

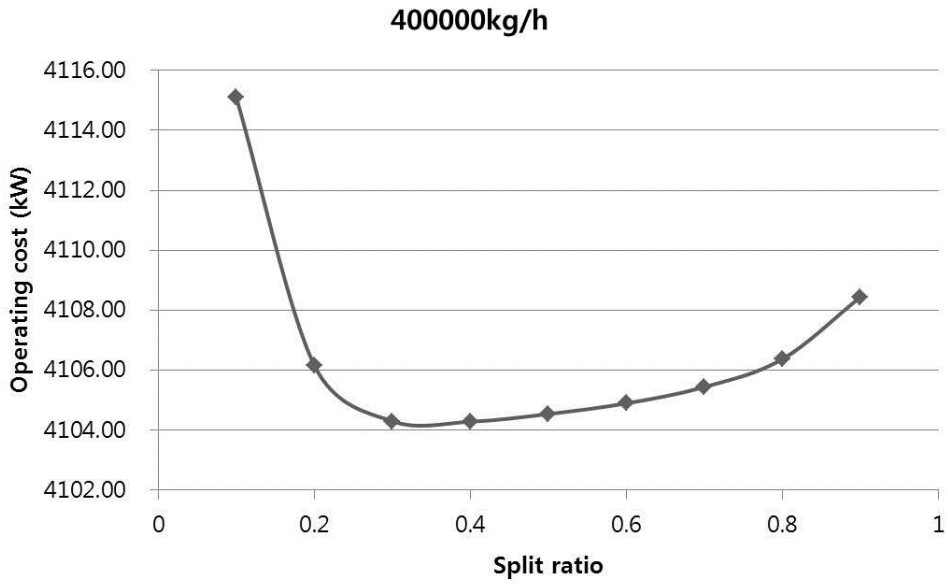

Figure 5- 12. The operating cost due to the varying split ratio at send-out rate of 400,000 kg/h.

When the split ratio ranges from 0.2 to 0.8, the split ratio had little effect on the operating costs. The optimal split ratio was determined for each send-out rate based on the results of the sensitivity analysis shown in Table 5-6. The energy saving cost was calculated by the subtracting operating cost of the proposed design, in which the send-out rate and split ratio changed, from the operating cost of the base design, in which the send-out rate changed. Figure 5-13 presents the energy saving ratio and cost according to the send-out rate at the optimal split ratio. The energy saving ratio decreases with increasing the send-out rate since the operating cost ratio of the BOG compressor to total process decrease; the proposed design mainly reduce the operating energy of the BOG compressor. However, the energy saving cost increases with the send-out rate since the cooling effects of the LNG stream increases with the send-out rate.

Table 5- 6. The optimal split ratio according to the send-out rate.

Send-out flow rate(kg/h)	Optimal split ratio	Energy saving ratio (%)
220,000	0.48	31.9
240,000	0.46	31.4
260,000	0.48	30.9
280,000	0.52	30.4
300,000	0.43	29.9
320,000	0.44	29.4
340,000	0.46	29.0
360,000	0.39	28.5
380,000	0.40	28.1
400,000	0.36	27.7
600,000	0.38	24.0
800,000	0.27	21.3
1,000,000	0.28	19.2
1,200,000	0.25	17.6
1,400,000	0.26	16.3

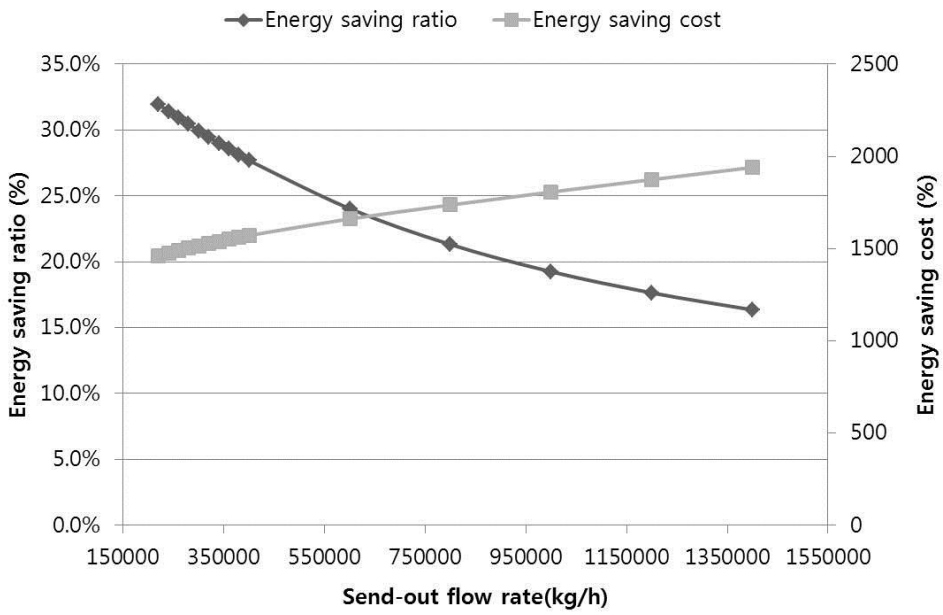

Figure 5- 13. The energy saving cost and ratio according to the send-out rate.

5.16.26. Profitability of the proposed design

Profitability of the proposed design was based on the regular send-out rate of 720 t/h presented in Table 5-7. The electric rate was assumed as $0.048/kWh. The energy saving of 1,698 kW was calculated using the difference in operating duties of base case design and retrofit design under the regular send-out condition of 720t/h. The equipment cost of the heat exchangers were only considered as the capital cost. The proposed design provides a 22.7% energy saving ratio and a 0.176 year payback period.

Table 5- 7. Profitability of the proposed design based on the regular send-out rate.

Profitability	Value
Energy saving ratio (%)	22.67
Energy saving cost (kW)	1,698
Energy saving cost ($/y)	716,844
Heat exchanger cost ($)	126,448
Payback period (year)	0.176

CHAPTER 6 : Conclusion and Future Works

6.17. Conclusion

This thesis has addressed the modeling and optimal design for LNG value chain, especially for liquefaction plant and LNG receiving terminal.

First, a steady-state modeling and simulation for natural gas liquefaction plant using double-expander nitrogen process was developed. Then, a simulation-based optimization methodology was proposed with case study using the developed model of double-expander process. The main concept was to develop a short-cut data-driven model. The method included comprehensive data extraction phase of the process in pre-specified operating range. The design space of the process was modeled using empirical modeling technique such as artificial neural network. The performance of the proposed method was shown by case study of natural gas liquefaction plant for floating production, storage and offloading unit (FPSO).

Natural gas liquefaction plant for offshore application requires nonflammable refrigerants for safety issues. For offshore natural gas production, it is appreciated that the use of hydrocarbons as refrigerants poses a safety issue. Therefore, a novel process of natural gas liquefaction for floating LNG was developed using nonflammable refrigerants only. Existing processes include reverse Brayton process with nitrogen as the working fluid and its derivatives. Pre-cooling with CO2 or HFC (hydro fluorocarbon) have also been proposed. Nitrous oxide has some advantages over carbon dioxide since the critical temperature is higher and triple point is lower. Especially, nitrous oxide can be utilized for liquefaction of natural gas at high pressure. A cascade process of N2O-N2O-N2 (pre-cooling, condensation, sub-

cooling) was designed for LNG production in this research. The proposed cycle is suitable for LNG-FPSO with low specific power comparable to mixed refrigerant processes.

Finally, a more efficient design of the boil-off gas (BOG) handling process was proposed based on a retrofit methodology to minimize the capital cost and operating cost. In order to develop the superstructure of the retrofit design, operating line of BOG handling process was thermodynamically analyzed. Based on the superstructure, the optimization problem of retrofit design was formulated. The retrofit design was optimized using the SQP (sequential quadratic programming) algorithm combined with process simulation. The results of the case study for the retrofit design provided energy saving of 1698 kW, equivalent to $716,844/y reduction of electricity cost. Payback period of the retrofit design was 0.176 years, which is sufficiently short for investment in the industry.

6.18. Future Works

Future studies about modeling and optimal design can be considerably extended and applied in LNG value chain because the phase change is the core concept in LNG related process design and operation. The in-depth analyses including process thermodynamics and operating conditions for natural gas liquefaction process will give an inspiration to design a new liquefaction process or draw design alternatives.

The proposed simulation-based optimization methodology can be applied for real-time optimization or data reconciliation. The production and consumption of LNG on a small scale is characterized by different dynamics compared to well-established large-scale LNG industry. Process design of liquefaction cycles must consider balance of criteria such as efficiency, layout, simplicity, safety, modularization, etc.

As the BOG handling is the key issue in LNG terminal operation, suggested retrofit methodology can give valuable clue for terminal operation enhancing process efficiency. Cryogenic energy recovery and optimization of BOG handling process can be further applied for LNG carriers.

Lastly, modeling and optimal design technique introduced in this thesis can be extended to the application of other cryogenic processes such as air separation industry and CO_2 liquefaction.

Literature Cited

[1] Administration EI. International Energy Outlook 2013 With Projections to 2040: Government Printing Office, 2013.

[2] Birol F, Corben J, Argiri M, Baroni M, Corbeau A, Cozzi L, et al. Are we entering a golden age of gas? IEA World Energy Outlook. 2011.

[3] Liss W. Demand outlook: A golden age of natural gas. Chemical Engineering Progress. 2012;108(8):35-40.

[4] Song K, Lee S, Shin S, Lee HJ, Han C. Simulation-based optimization methodology for offshore natural gas liquefaction process design. Industrial & Engineering Chemistry Research. 2014;53(13):5539-44.

[5] Kidnay AJ, Parrish WR. Fundamentals of natural gas processing: CRC Press, 2006.

[6] Wood D, Mokhatab S, Economides MJ. Offshore natural gas liquefaction process and development issues. SPE Projects Facilities & Construction. 2007;2(04):1-7.

[7] Shimamura Y. FPSO/FSO: State of the art. Journal of marine science and technology. 2002;7(2):59-70.

[8] Finn A. Are floating LNG facilities viable options? HYDROCARBON PROCESSING. 2009;88(7):31-+.

[9] Li Q, Ju Y. Design and analysis of liquefaction process for offshore associated gas resources. Applied Thermal Engineering. 2010;30(16):2518-25.

[10] Sheffield JA. Offshore LNG Production-How to Make it Happen. LNG Review

2005. 2005.

[11] Shukri T, Barclay M, Consultants L, Energy FW. Single mixed refrigerant process has appeal for growing offshore market. LNG Journal. 2007;3:31-7.

[12] Finn AJ, Johnson GL, Tomlinson TR. LNG technology for offshore and midscale plants. Conference LNG technology for offshore and midscale plants.

[13] Finn A. Effective LNG production offshore. Conference Effective LNG production offshore. p. 10-3.

[14] Memon MK, Tunio SQ, Memon KR, Lashari AA. A Comparative Study of Liquefied Natural Gas: An Overview. 2014.

[15] Choi MS. Floating LNG is Coming of Age. Conference Floating LNG is Coming of Age. Offshore Technology Conference.

[16] Bukowski J. Natural gas liquefaction technology for floating LNG facilities. Conference Natural gas liquefaction technology for floating LNG facilities.

[17] Moran MJ, Shapiro HN, Boettner DD, Bailey M. Fundamentals of engineering thermodynamics: John Wiley & Sons, 2010.

[18] Venkatarathnam G. Cryogenic mixed refrigerant processes: Springer, 2008.

[19] Gaumer Jr LS, Newton CL. Combined cascade and multicomponent refrigeration system and method. US Patent 3,763,658; 1973.

[20] Andress D, Watkins R. Beauty of simplicity: Phillips optimized cascade LNG liquefaction process. Conference Beauty of simplicity: Phillips optimized cascade LNG liquefaction process, vol. 710. AIP Publishing, p. 91-100.

[21] Wilkes MA. Floating LNG liquefaction facilities using the optimized cascade

process. Conference Floating LNG liquefaction facilities using the optimized cascade process, vol. 91.

[22] Bradley A, Duan H, Elion W, van Soest-Vercammen E, Nagelvoort RK. Innovation in the LNG industry: Shell's approach. Conference Innovation in the LNG industry: Shell's approach. p. 5-9.

[23] Jensen JB, Skogestad S. Optimal operation of a mixed fluid cascade LNG plant. Computer Aided Chemical Engineering. 2006;21:1569-74.

[24] Finn A, Johnson G, Tomlinson T. Developments in natural gas liquefaction. Hydrocarbon processing. 1999;78(4):47-56.

[25] Barclay M, Shukri T, Consultants L. Enhanced single mixed refrigerant process for stranded gas liquefaction. Conference Enhanced single mixed refrigerant process for stranded gas liquefaction.

[26] Price B. Small-scale LNG facility development: Include these vital design characteristics for improved project costs: Gas processing developments. Hydrocarbon processing. 2003;82(1):37-9.

[27] Bukowski J, Liu YN, Boccella MS, Kowalski LJ. Innovations in natural gas liquefaction technology for future LNG plants and floating LNG facilities. IGRC, Seoul, October. 2011.

[28] Lam HL, Klemeš JJ, Kravanja Z, Varbanov PS. Software tools overview: process integration, modelling and optimisation for energy saving and pollution reduction. Asia-Pacific Journal of Chemical Engineering. 2011;6(5):696-712.

[29] Smith J, Van Ness H, Abbott M. Chemical engineering thermodynamics.

McGraw-Hill, NY. 2001.

[30] Peng D-Y, Robinson DB. A new two-constant equation of state. Industrial & Engineering Chemistry Fundamentals. 1976;15(1):59-64.

[31] Soave G. Equilibrium constants from a modified Redlich-Kwong equation of state. Chemical Engineering Science. 1972;27(6):1197-203.

[32] Prausnitz JM, Lichtenthaler RN, de Azevedo EG. Molecular thermodynamics of fluid-phase equilibria: Pearson Education, 1998.

[33] Dubar CA, Tu OLM. Liquefaction apparatus. Google Patents; 2001.

[34] Jensen JB, Skogestad S. Steady-state operational degrees of freedom with application to refrigeration cycles. Industrial & Engineering Chemistry Research. 2009;48(14):6652-9.

[35] Wang M, Zhang J, Xu Q, Li K. Thermodynamic-analysis-based energy consumption minimization for natural gas liquefaction. Industrial & Engineering Chemistry Research. 2011;50(22):12630-40.

[36] Shah NM, Hoadley AF. A targeting methodology for multistage gas-phase auto refrigeration processes. Industrial & engineering chemistry research. 2007;46(13):4497-505.

[37] Cao W-s, Lu X-s, Lin W-s, Gu A-z. Parameter comparison of two small-scale natural gas liquefaction processes in skid-mounted packages. Applied Thermal Engineering. 2006;26(8):898-904.

[38] Song K, Jeong C, Nam J, Han C. Hybrid compressor model for optimal operation of compressed dry air system in LCD production industry. Industrial & Engineering

Chemistry Research. 2012;51(13):4998-5002.

[39] Singh K, Shenoy K, Mahendra A, Ghosh S. Artificial neural network based modelling of head and power characteristics of pump-mixer. Chemical engineering science. 2004;59(14):2937-45.

[40] Fissore D, Barresi AA, Manca D. Modelling of methanol synthesis in a network of forced unsteady-state ring reactors by artificial neural networks for control purposes. Chemical engineering science. 2004;59(19):4033-41.

[41] Kadlec P, Gabrys B, Strandt S. Data-driven soft sensors in the process industry. Computers & Chemical Engineering. 2009;33(4):795-814.

[42] Becker T, Enders T, Delgado A. Dynamic neural networks as a tool for the online optimization of industrial fermentation. Bioprocess and Biosystems Engineering. 2002;24(6):347-54.

[43] Nielsen D, Pitchumani R. Intelligent model-based control of preform permeation in liquid composite molding processes, with online optimization. Composites Part A: Applied Science and Manufacturing. 2001;32(12):1789-803.

[44] Gonzaga J, Meleiro L, Kiang C, Maciel Filho R. ANN-based soft-sensor for real-time process monitoring and control of an industrial polymerization process. Computers & Chemical Engineering. 2009;33(1):43-9.

[45] Rotem Y, Wachs A, Lewin D. Ethylene compressor monitoring using model-based PCA. AIChE Journal. 2000;46(9):1825-36.

[46] Chang H-M, Chung MJ, Lee S, Choe KH. An efficient multi-stage Brayton–JT cycle for liquefaction of natural gas. Cryogenics. 2011;51(6):278-86.

[47] Remeljej C, Hoadley A. An exergy analysis of small-scale liquefied natural gas (LNG) liquefaction processes. Energy. 2006;31(12):2005-19.

[48] Lee S, Long NVD, Lee M. Design and optimization of natural gas liquefaction and recovery processes for offshore floating liquefied natural gas plants. Industrial & Engineering Chemistry Research. 2012;51(30):10021-30.

[49] Taleshbahrami H, Saffari H. OPTIMIZATION OF THE C 3 MR CYCLE WITH GENETIC ALGORITHM. Transactions of the Canadian Society for Mechanical Engineering. 2010;34(3-4):433.

[50] Alabdulkarem A, Mortazavi A, Hwang Y, Radermacher R, Rogers P. Optimization of propane pre-cooled mixed refrigerant LNG plant. Applied thermal engineering. 2011;31(6):1091-8.

[51] Geladi P, Kowalski BR. Partial least-squares regression: a tutorial. Analytica chimica acta. 1986;185:1-17.

[52] Bulsari A. Neural networks for chemical engineers: Elsevier Science Inc., 1995.

[53] Himmelblau DM. Applications of artificial neural networks in chemical engineering. Korean Journal of Chemical Engineering. 2000;17(4):373-92.

[54] Baş D, Boyacı İH. Modeling and optimization I: Usability of response surface methodology. Journal of Food Engineering. 2007;78(3):836-45.

[55] Baş D, Boyacı İH. Modeling and optimization II: Comparison of estimation capabilities of response surface methodology with artificial neural networks in a biochemical reaction. Journal of Food Engineering. 2007;78(3):846-54.

[56] Bezerra MA, Santelli RE, Oliveira EP, Villar LS, Escaleira LA. Response surface

methodology (RSM) as a tool for optimization in analytical chemistry. Talanta. 2008;76(5):965-77.

[57] Box GE, Behnken DW. Some new three level designs for the study of quantitative variables. Technometrics. 1960;2(4):455-75.

[58] Box GE, Wilson K. On the experimental attainment of optimum conditions. Journal of the Royal Statistical Society Series B (Methodological). 1951;13(1):1-45.

[59] Hwang J-H, Roh M-I, Lee K-Y. Determination of the optimal operating conditions of the dual mixed refrigerant cycle for the LNG FPSO topside liquefaction process. Computers & Chemical Engineering. 2013;49:25-36.

[60] Won W, Lee SK, Choi K, Kwon Y. Current trends for the floating liquefied natural gas (FLNG) technologies. Korean Journal of Chemical Engineering. 2014;31(5):732-43.

[61] Barclay M, Gongaware D, Dalton K, Skrzypkowski M. Thermodynamic cycle selection for distributed natural gas liquefaction. Conference Thermodynamic cycle selection for distributed natural gas liquefaction, vol. 710. AIP Publishing, p. 75-82.

[62] Dubar CA. Liquefaction process. Google Patents; 1998.

[63] Neeraas BO, Sandvik TE. Dual nitrogen expansion process. Google Patents; 2009.

[64] Fredheim AO, Paurola P. Natural gas liquefaction process. Google Patents; 2008.

[65] https://go.sitehawk.com/msds/viewimage.aspx?MaterialID=623520&facilityID=1336&UseCatalog=True

[66] http://encyclopedia.airliquide.com/encyclopedia.asp?languageid=11&GasID=

55&CountryID=19#MajorApplications

[67] Aspelund A, Gundersen T, Myklebust J, Nowak M, Tomasgard A. An optimization-simulation model for a simple LNG process. Computers & Chemical Engineering. 2010;34(10):1606-17.

[68] Kim J-K, Lee GC, Zhu FX, Smith R. Cooling system design. Heat transfer engineering. 2002;23(6):49-61.

[69] Wu G, Zhu X. Design of integrated refrigeration systems. Industrial & engineering chemistry research. 2002;41(3):553-71.

[70] Lee G, Smith R, Zhu X. Optimal synthesis of mixed-refrigerant systems for low-temperature processes. Industrial & engineering chemistry research. 2002;41(20):5016-28.

[71] Vaidyaraman S, Maranas CD. Synthesis of mixed refrigerant cascade cycles. Chemical Engineering Communications. 2002;189(8):1057-78.

[72] Nogal FD, Kim J-K, Perry S, Smith R. Optimal design of mixed refrigerant cycles. Industrial & Engineering Chemistry Research. 2008;47(22):8724-40.

[73] Hasan M, Jayaraman G, Karimi I, Alfadala H. Synthesis of heat exchanger networks with nonisothermal phase changes. AIChE journal. 2010;56(4):930-45.

[74] Hatcher P, Khalilpour R, Abbas A. Optimisation of LNG mixed-refrigerant processes considering operation and design objectives. Computers & Chemical Engineering. 2012;41:123-33.

[75] Lim W, Choi K, Moon I. Current status and perspectives of liquefied natural gas (LNG) plant design. Industrial & Engineering Chemistry Research. 2013;52(9):3065-

88.

[76] Khan MS, Lee S, Lee M. Optimization of single mixed refrigerant natural gas liquefaction plant with nonlinear programming. Asia-Pacific Journal of Chemical Engineering. 2012;7(S1):S62-S70.

[77] Hwang J-H, Ku N-K, Roh M-I, Lee K-Y. Optimal Design of Liquefaction Cycles of Liquefied Natural Gas Floating, Production, Storage, and Offloading Unit Considering Optimal Synthesis. Industrial & Engineering Chemistry Research. 2013;52(15):5341-56.

[78] Vink K, Nagelvoort RK. Comparison of baseload liquefaction processes. Conference Comparison of baseload liquefaction processes, vol. 3.

[79] Park C, Song K, Lee S, Lim Y, Han C. Retrofit design of a boil-off gas handling process in liquefied natural gas receiving terminals. Energy. 2012;44(1):69-78.

[80] Park C, Lee C-J, Lim Y, Lee S, Han C. Optimization of recirculation operating in liquefied natural gas receiving terminal. Journal of the Taiwan Institute of Chemical Engineers. 2010;41(4):482-91.

[81] Shin MW, Shin D, Choi SH, Yoon ES, Han C. Optimization of the operation of boil-off gas compressors at a liquified natural gas gasification plant. Industrial & Engineering Chemistry Research. 2007;46(20):6540-5.

[82] Querol E, Gonzalez-Regueral B, García-Torrent J, García-Martínez M. Boil off gas (BOG) management in Spanish liquid natural gas (LNG) terminals. Applied Energy. 2010;87(11):3384-92.

[83] Lee S, Yang Y-m. Operating information system for LNG facilities. Conference

Operating information system for LNG facilities. p. 363-76.

[84] Lee C-J, Lim Y, Park C, Lee S, Han C. Synthesis of unloading operation procedure for a mixed operation of above-ground and in-ground liquefied natural gas storage tanks using dynamic simulation. Industrial & Engineering Chemistry Research. 2010;49(17):8219-26.

[85] Kim D, Ha Y, Park I, Yoon Y, Baek Y. Study on the improvement of BOG recondensation process at LNG receiving terminal. KIGAS. 2001;5(3):23-8.

[86] Lim Y, Lee C-J, Lee S, Park C, Han C. Methodology for stable dynamic simulation of a LNG pipe under two-phase-flow generation. Industrial & Engineering Chemistry Research. 2010;49(18):8587-92.

[87] Jang N, Shin MW, Choi SH, Yoon ES. Dynamic simulation and optimization of the operation of boil-off gas compressors in a liquefied natural gas gasification plant. Korean Journal of Chemical Engineering. 2011;28(5):1166-71.

[88] Liu C, Zhang J, Xu Q, Gossage JL. Thermodynamic-analysis-based design and operation for boil-off gas flare minimization at LNG receiving terminals. Industrial & Engineering Chemistry Research. 2010;49(16):7412-20.

[89] Dharmadhikari S. Optimize LNG vaporizers. Hydrocarbon processing. 2004;83(10):95-9.

[90] Yang C, Huang Z. Lower emission LNG vaporization. LNG journal. 2004;6:24-6.

[91] Liu H, You L. Characteristics and applications of the cold heat exergy of liquefied natural gas. Energy conversion and management. 1999;40(14):1515-25.

[92] Qiang W, Yanzhong L, Jiang W. Analysis of power cycle based on cold energy of liquefied natural gas and low-grade heat source. Applied thermal engineering. 2004;24(4):539-48.

[93] Qiang W, Yanzhong L, Xi C. Exergy analysis of liquefied natural gas cold energy recovering cycles. International journal of energy research. 2005;29(1):65-78.

[94] Sun W, Hu P, Chen Z, Jia L. Performance of cryogenic thermoelectric generators in LNG cold energy utilization. Energy conversion and management. 2005;46(5):789-96.

[95] Kim H, Hong S. Review on economical efficiency of LNG cold energy use in South Korea. Conference Review on economical efficiency of LNG cold energy use in South Korea.

[96] Szargut J, Szczygiel I. Utilization of the cryogenic exergy of liquid natural gas (LNG) for the production of electricity. Energy. 2009;34(7):827-37.

[97] Deng S, Jin H, Cai R, Lin R. Novel cogeneration power system with liquefied natural gas (LNG) cryogenic exergy utilization. Energy. 2004;29(4):497-512.

[98] Cho H, Shah S, Lim K. Case history for gas re-liquefaction system at the Pyeongtaek LNG terminal, South Korea. Proceedings of Gastech 2000. 2000.

[99] Jung M-J, Cho JH, Ryu W. LNG terminal design feedback from operator's practical improvements. Conference LNG terminal design feedback from operator's practical improvements.

[100] Lim G-H, Park L-H. LNG terminal operator's design feedback and technical challenges. Proceedings of Gastech. 2005.

[101] Sohn Y. Basic design of Pyeongtaek LNG receiving terminal-II of Korea gas corporation. Conference Basic design of Pyeongtaek LNG receiving terminal-II of Korea gas corporation.

[102] Hasan MF, Zheng AM, Karimi I. Minimizing boil-off losses in liquefied natural gas transportation. Industrial & Engineering Chemistry Research. 2009;48(21):9571-80.

[103] Seider WD, Seader JD, Lewin DR. PRODUCT & PROCESS DESIGN PRINCIPLES: SYNTHESIS, ANALYSIS AND EVALUATION, (With CD): John Wiley & Sons, 2009.

Abstract in Korean (요약)

천연가스는 가장 빠르게 사용량이 급증하고 있는 화석 연료로서 특히 청정성과 경제성으로 인하여 발전 및 산업 분야에서 널리 사용되고 있다. 전 세계 천연가스 무역량은 2010년에 약 1조 입방 미터였으나 2020년경에는 1.5조 및 2030년이 되면 2조 입방 미터로 2배가 될 것으로 예상된다. 특히 천연가스를 액화하여 액화천연가스 (LNG) 형태로 수송되는 양이 급격히 늘어날 것으로 예상된다.

액화천연가스 가치사슬의 핵심은 바로 원거리로의 이송을 가능하게 하는 액체로의 상 변화에 있다. 공급 측면의 천연가스 생산 공정과 수요 측면의 터미널 공정은 고비용 구조로 액화천연가스 가치사슬의 핵심에 해당한다. 본 논문은 천연가스 액화공정과 인수기지에서의 재기화 공정에 대한 모델링과 최적 설계를 제시하였다.

본 논문은 네 개의 주요한 부분으로 구성된다. 첫째, 액화 플랜트의 모델링과 시뮬레이션이 수행되었다. 둘째, 시뮬레이터의 장점을 최대한 활용하면서도 경험 기반 모델링을 통해 공정을 사상하여 최적화를 가능하게 한 새로운 방법론을 제시하였다. 또한 개발된 방법론을 질소 팽창 공정에 적용하여 그 효과를 입증하였다. 셋째, 부유식 해상 플랜트에 적용하기 위해 비 휘발성 물질을 냉매로 이용한 신 천연가스 액화 공정을 설계하였다. 기존 혼합 냉매를 이용한 공정은 효율적이나 많은 양의 휘발성 물질 저장 탱크를 수반하는 것이 단점으로 지적되었다.

개발된 공정은 N2O-N2O-N2 다단 공정으로 비 휘발성 물질인 아산화질소와 질소 만을 이용하면서도 기존 혼합 냉매 공정과 비슷한 효율을 갖는 장점이 있다. 마지막으로 천연가스 터미널에서 재기화 공정의 개선된 설계를 제시하여 에너지 절감을 이루었다. 액화천연가스의 냉열을 활용하여 열교환 합성을 통해 기존 공정을 개선하는 방법론을 제시하였다.

주요어: 공정 설계, 최적화, 천연가스, 액화천연가스, 액화 플랜트, 액화천연가스 인수기지

학번: 2008-21083
성명: 송기욱